МІНІСТЕРСТВО ОСВІТИ ТА НАУКИ УКРАЇНИ
Національний авіаційний університет
Кафедра конструкції літальних апаратів

ДОПУСТИТИ ДО ЗАХИСТУ
Завідувач кафедри, д.т.н., проф.
_____ Сергій ІГНАТОВИЧ
«___» _____ 2023 р.

КВАЛІФІКАЦІЙНА РОБОТА
ЗДОБУВАЧА ОСВІТНЬОГО СТУПЕНЯ
«БАКАЛАВР»

Тема: «Аванпроект пасажирського літака із застосуванням нанотехнологій»

Виконав: _____ **Неоніла ЮРЧЕНКО**

Керівник: к.т.н., доц. _____ **Володимир КРАСНОПОЛЬСЬКИЙ**

Нормоконтролер: к.т.н., доц. _____ **Володимир КРАСНОПОЛЬСЬКИЙ**

Київ 2023

MINISTRY OF EDUCATION AND SCIENCE OF UKRAINE
National Aviation University
Department of Aircraft Design

PERMISSION TO DEFEND
Head of the department,
Professor, Dr. of Sc.
_____ Sergiy IGNATOVYCH
"___" _____ 2023

BACHELOR DEGREE THESIS

Topic: "Preliminary design of passenger aircraft with application of nanotechnologies"

Fulfilled by: _____ **Neonila YURCHENKO**

Supervisor:
PhD, associate professor _____ **Volodymyr KRASNOPOLSKYI**

Standards inspector
PhD, associate professor _____ **Volodymyr KRASNOPOLSKYI**

Kyiv 2023

НАЦІОНАЛЬНИЙ АВІАЦІЙНИЙ УНІВЕРСИТЕТ

Аерокосмічний факультет
Кафедра конструкції літальних апаратів
Освітній ступінь «Бакалавр»
Спеціальність 134 «Авіаційна та ракетно-космічна техніка»
Освітньо-професійна програма «Обладнання повітряних суден»

ЗАТВЕРДЖУЮ
Завідувач кафедри, д.т.н, проф.
_____ Сергій ІГНАТОВИЧ
«___» _____ 2023 р.

ЗАВДАННЯ

на виконання кваліфікаційної роботи здобувача вищої освіти

ЮРЧЕНКО НЕОНІЛИ ВОЛОДИМИРІВНИ

1. Тема роботи: «Аванпроект пасажирського літака із застосуванням нанотехнологій», затверджена наказом ректора від 1 травня 2023 року №815/ст.

2. Термін виконання проекту: з 29 травня 2023 р. по 25 червня 2023 р.

3. Вихідні дані до проекту: максимальна кількість пасажирів 185, дальність польоту з максимальним комерційним навантаженням 5700 км, крейсерська швидкість польоту 870 км/год, висота польоту 10 км.

4. Зміст пояснювальної записки: вступ, основна частина, обґрунтування вихідних даних для розрахунку, розрахунок геометричних параметрів літака та центрування, спеціальна частина.

5. Перелік обов’язкового графічного матеріалу: загальний вигляд літака (А1×1), компонувальне креслення фюзеляжу (А1×1), схеми і діаграми з Catia V5.

6. Календарний план-графік:

№	Завдання	Термін виконання	Відмітка про виконання
1	Вибір вихідних даних, аналіз льотно-технічних характеристик літаків-прототипів.	29.05.2023 – 31.05.2023	
2	Вибір та розрахунок параметрів проєктованого літака.	01.06.2023 – 03.06.2023	
3	Виконання компонування літака та розрахунок його центрування.	04.06.2023 – 05.06.2023	
4	Розробка креслень по основній частині дипломної роботи.	06.06.2023 – 07.06.2023	
5	Огляд літератури за проблематикою роботи.	08.06.2023 – 09.06.2023	
6	Створення 3д моделі крила	10.06.2023 – 11.06.2023	
7	Оформлення пояснювальної записки та графічної частини роботи.	12.06.2023 – 14.06.2023	
8	Подача роботи для перевірки на плагіат.	15.06.2023 – 18.06.2023	
9	Попередній захист кваліфікаційної роботи.	19.06.2023	
10	Виправлення зауважень. Підготовка супровідних документів та презентації доповіді.	20.06.2023 – 22.06.2023	
11	Захист дипломної роботи.	23.06.2023 – 25.06.2023	

7. Дата видачі завдання: 29 травня 2023 року

Керівник кваліфікаційної роботи _____ Володимир КРАСНОПОЛЬСЬКИЙ

Завдання прийняв до виконання _____ Неоніла ЮРЧЕНКО

NATIONAL AVIATION UNIVERSITY

Aerospace Faculty
Department of Aircraft Design
Educational Degree "Bachelor"
Specialty 134 "Aviation and Aerospace Technologies"
Educational Professional Program "Aircraft Equipment"

APPROVED BY
Head of Department,
Professor Dr. of Sc.
_____ Sergiy IGNATOVYCH
"___" _____ 2023

TASK

for the bachelor degree thesis

Neonila YURCHENKO

1. Topic: "Preliminary design of the mid-range passenger aircraft with 185 passenger capacity" approved by the Rector's order №815/ст. "21" May 2023 year.
2. Period of work: since 29 May 2023 till 25 June 2023.
3. Initial data for the project: maximum number of passengers 185, cruise speed V_{cr} = 870 km/h, flight range with maximum commercial load L = 5700 km, operating altitude H_{op} = 10 km.
4. The content of the explanatory note: introduction, the main part, the justification of the initial data for the calculation, the calculation of the geometric parameters of the aircraft and centering, the special part.
5. Required material: general view of the airplane (A1×1), layout of the airplane (A1×1), schemes and diagrams of Catia V5.

6. Thesis schedule:

№	Task	Time limits	Done
1	Selection of initial data, analysis of flight technical characteristics of prototypes aircrafts.	29.05.2023 – 31.05.2023	
2	Selection and calculation of the aircraft designed parameters.	01.06.2023 – 03.06.2023	
3	Performing of aircraft layout and centering calculation.	04.06.2023 – 05.06.2023	
4	Development of drawings on the thesis main part.	06.06.2023 – 07.06.2023	
5	Inspection of the literature behind the problem of work.	08.06.2023 – 09.06.2023	
6	Creating a 3D wing model	10.06.2023 – 11.06.2023	
7	Explanatory note checking, editing, preparation of the diploma work graphic part.	12.06.2023 – 14.06.2023	
8	Submission of the work to plagiarism check.	15.06.2023 – 18.06.2023	
9	Preliminary defense of the thesis.	19.06.2023	
10	Making corrections, preparation of documentation and presentation.	20.06.2023 – 22.06.2023	
11	Defense of the diploma work.	23.06.2023 – 25.06.2023	

7. Date of the task issue: 29 May 2023

Supervisor: _____ Volodymyr KRASNOPOLSKYI

Student: _____ Neonila YURCHENKO

РЕФЕРАТ

Пояснювальна записка кваліфікаційної роботи бакалавра «Аванпроект пасажирського літака із застосуванням нанотехнологій»:

72 с., 19 рис., 8 табл., 13 джерел

Дана кваліфікаційна робота присвячена розробці середньомагістрального пасажирського літака на 185 пасажирів, що відповідає міжнародним стандартам польотів, стандартам безпеки, економічності та надійності, а також пошуку прктичних методів використання нанотехнологій в авіаційній галузі.

В роботі були використані аналітичні розрахунки, комп'ютерне проєктування з використанням систем CAD/CAM/CAE і ескізне проєктування.

Результати кваліфікаційної роботи мають практичне значення, оскільки вони можуть бути використані для підвищення надійності та результативності перевезень пассажирів повітряним транспортом, а також розширення можливостей боротьби від обледеніння літака.

Вміст кваліфікаційної роботи може бути використаний в освітньому процесі та практичній роботі фахівців-конструкторів в спеціалізованих проєктних установах.

Дипломна робота, аванпроєкт літака, компонування, центрування, нанотехнології, розрахунок паливної ефективності

ABSTRACT

Bachelor degree thesis "Preliminary design of passenger aircraft with application of nanotechnologies"

72 pages, 19 figures, 8 tables, 13 references

This qualification work is devoted to the development of a medium-haul passenger plane for 185 passengers that meets international flight standards, standards of safety, economy and reliability, as well as the search for practical methods of using nanotechnology in the aviation industry.

Analytical calculations, computer-aided design using CAD/CAM/CAE systems, and sketch design were used in the work.

The results of the qualification work are of practical importance, as they can be used to increase the reliability and effectiveness of passenger transportation by air transport, as well as to expand the possibilities of elimination aircraft icing.

The content of the qualification work can be used in the educational process and practical work of design specialists in specialized design institutions.

Bachelor thesis, preliminary design, cabin layout, center of gravity, nanotechnology, fuel efficiency calculation

Format	№	Designation	Name	Quantity	Notes
			General documents		
A4	1	NAU 23 12Y 00 00 00 43 TW	Task for work	1	
	2	NAU 23 12Y 00 00 00 43	Mid-range passenger aircraft	2	
A1		Sheet 1	General view		
A1		Sheet 2	Fuselage layout		
A4	3	NAU 23 12Y 00 00 00 43 EN	Mid-range passenger aircraft	72	
			Explanatory note		
			Documentation for assembly units		
A1	4	NAU 23 12Y 00 00 00 43	Nanofilm design	1	

					NAU 23 12Y 00 00 00 43 EN
	Sh.	№ doc.	Sign	Date	
Done by		Yurchenko N.V.			Preliminary design of passenger aircraft with application of nanotechnologies (List of diploma work)
Supervisor		Krasnopolskyi V.S.			
St.control.		Krasnopolskyi V.S.			
Head of dep.		Ignatovich S.R.			

list	sheet	sheets
Q	9	72

402 ASF 134

CONTENT

INTRODUCTION

Human life has become many times easier since the moment when everyone was given the opportunity to travel between cities and countries using an airplane. Every year the demand for aircraft is growing exponentially. This is due not only to the rise of developing countries, but also to the decline in the economic cost of air travel. An airplane will get to anywhere in the world much faster than a train or a ship, which is why most people prefer the transport that will take them to point b as soon as possible. The main disadvantage is the high price of tickets, so many passengers prefer to use trains whose cost in several times less.

Taking into account the demand for medium-haul passenger transportation, it was decided to design just such an aircraft. A distinctive feature of a passenger plane compared to a cargo plane is the need to create the most favorable conditions for the comfort and safety of passengers. If in a cargo plane there is a calculation for capacity, then in a passenger plane it is worth taking care of people. The passenger will always prefer the most comfortable conditions, so the need to ensure comfort and safety comes first.

After reviewing different aircrafts, their capacity, flight range and other facts, it was decided to design an aircraft for 185 people with a flight range of 5700 kilometers with a maximum payload. Airbus A320neo, COMAC-C919 and Airbus A320 were taken as prototypes. Airbus A320neo is a deep modernization of the family of narrow-body medium-haul airliners and it is also the main prototype. In fact, this is an updated version of the well-known A320, but with less noise and more efficiency.

The prototypes were chosen not only on the basis of their similarity in many respects, but also on the basis of their popularity in the market. The purpose of the work is to isolate the best that is in these models and design a comfortable, economical aircraft so that people have a desire to buy a ticket for.

1. PRELIMINARY DESIGN OF MID-RANGE AIRCRAFT

1.1 Analysis of prototypes and short description of designed aircraft

Each aircraft has its own parameters that meet the requirements of not only the quality of the aircraft, but also its safety. Therefore, it is necessary to choose the parameters that will be responsible for all the characteristics of the aircraft. It is necessary that the layout is responsible for the entire complex of flight performance, weight, geometric, aerodynamic and economic characteristics. The analysis of various prototypes helped to isolate the exact initial data for starting work on the project.

Detailed statistical information regarding these prototypes in Table 1.1.

Table 1.1

Operational-technical data of prototypes

Performance / **Aircraft**	A320neo	COMAC-C919	A320	Designed aircraft
1	2	3	4	5
Crew/flight attendance, persons	2/5	2/5	2/4	2/5
Maximum take-off mass, [kg]	79000	72500	77000	99035
Commercial payload, $m_{c.p.}$, [kg]	11850	14500	11550	19332.5
Cruising speed $V_{c.s.}$, [km/h]	828	834	828	870
Cruising altitude, [m]	12.1	12	11.9	10
Flight range, [km]	6300	4075	6150	5700
Spesific wing load, [kPa]	5.12	3.18	4.9	6.5
Thrust to weight ratio, [N/kg]	0.0030	0.0035	0.0029	0.0023
Take-off distance, $L_{t.d.}$, [m]	1 951	2 052	1 828	1 892
Landing distance, $L_{l.d.}$, [m]	1600	1600	1230	1308
Landing speed V_{ls}, [km/h]	250	250	260	148.9

Ending of the Table 1.1

1	2	3	4	5
Commercial payload ratio, [%]	15	20	15	15
Number and type of engines	2× Pratt &Whitney PW1100G	2× (CFMInternationa l LEAP-1C)	2× (CFM56-5B)	2× Pratt &Whitney PW1100G
Take-off thrust [kN]	120	120	120	120
Cruising thrust [kN]	98	98	98	98
Pressure ratio	50:1	50:1	28:1	50:1
Bypass ratio	11:1	11:1	6:1	11:1
Fuselage diameter, [m]	3.95	3.96	3.96	4.2
Fineness ratio	9.51	9.82	9.5	9
Wing sweepback angle 1/4 chord, °	25	25	25	32
Aspect ratio	9.39	8.74	9.50	9.4
Taper ratio	2.4	2.5	3.27	3.4
Airfiol thickness	11.5	13	15.2	11
HTU span, [m]	16.18	14.7	15.85	16
HTU taper ratio	0.3	0.25	0.3	0.25
HTU aspect ratio	4.4	6	4.4	8.5
HTU sweepback angle 1/4 chord, °	28	30	28	30
VTU span, [m]	11.8	13.67	11.8	13.11
VTU taper ratio	0.38	0.25	0.3	0.3
VTU aspect ratio	1.7	0.25	1.7	0.22
VTU sweepback angle °	30	35	33	40
Wheel base, [m]	16.9	13.47	12.64	14.69
Whell track, [m]	7.59	7.62	7.59	7.93

Aircraft performance depends on both aerodynamic and operational characteristics, while it depends on the aerodynamic design and layout. To increase the demand for an aircraft, it is necessary to increase the safety of flights, its economy and the regularity of flights. That is why it is so important to choose the right aircraft layout.

1.2 Brief description of the main parts of the aircraft

All three prototypes are medium-haul passenger aircrafts and have similar characteristics. The main prototype is a modification of the A320, the "neo" prefix indicates that the aircraft is equipped with new engines (PW 1100G or CFM LEAP-1A) and a new type of wingtips. Thanks to the new engines, the modification is more economical, which increases the flight range, and the aircraft itself is much quieter both in the cabin and overboard. A320neo tends to have a statistical advantage over A320ceo. It's all about a higher cruising speed of Mach 0.82 (1,013 [km/h] or 629 [mph]), a higher payload capacity in two classes (150-180 passengers) and a longer range (6300 [km]/3400 [nm]) [1].

The prototype COMAC C919 has a length of 38.9 [m], a height of 11.95 [m] and a wingspan of 35.8 [m]. The fuselage is 4.16 [m] high and 3.96 [m] wide [2]. In fact, its dimensions are almost identical to the A320. Passenger capacity is 168 people. Equipped with two FM International LEAP 1C engines. If we compare its flight range with the A320neo, then it is inferior to this modification (4075 [km]).

Wing

One of the parts of the aircraft that are most essential for flying. Most of the lift needed for flight comes from the airflow above the wings. In addition to the wing that emerge from the middle of the fuselage, there are also two smaller planes at the rear of most aircraft, namely the tail section. To improve the characteristics of take-off and landing, the wings are additionally equipped mechanisms. During the aircraft's take-off and landing, these components play a crucial role in managing its movement. They are responsible for regulating the aircraft's speed and controlling its performance during the take-off and landing phases. Some aircraft wing designs even incorporate fuel storage capacity.

While designing the aircraft, careful consideration was given to the possibility of optimizing its design in the future, including engine replacement or repair.

To enhance passenger visibility, a lower single-wing configuration was incorporated. Additionally, a proliferation device was integrated onto the wing to align with the design requirements. Dampers were installed on the wing to mitigate the

impact of shock waves on the flight. Moreover, the connection between the fuselage and wings was optimized to minimize drag effects in that area.

Apart from the main wing structure, there are two ailerons that enhance the aircraft's maneuverability. These are moving components, thanks to which it is possible to control the aircraft relative to the longitudinal axis. These elements operate synchronously. However, they deviate in different directions. When one tilts upwards, the other tilts downwards. The lifting force on the console, deflected upwards, decreases. Due to this, the rotation of the fuselage is carried out.

Fuselage

The fuselage is one of the main parts of an aircraft. It is a hollow tube, which is the body of the aircraft and is designed to hold passengers and cargo. There are different types of fuselage, but they all perform one of the main functions, connecting the main parts of the aircraft.

A semi-monocoque design is generally preferred, as this design does an excellent job of absorbing and transferring loads that occur during flight. Semi-monocoque fuselage consists of stringers or spars. These components form the longitudinal elements of the structure. Their purpose is to transfer axial loads that occur due to the bending of the fuselage under load. The stringers also support the skin and, in combination with the frames, create bays over which the skin is attached accordingly.

For the manufacture of working skin, the following materials are used: aluminum, composite materials, titanium and steel alloys, aircraft polywood.

Tail unit

The tail section is composed of the horizontal and vertical stabilizers, elevators, and rudder. It follows a standard design, with the horizontal tail featuring a reverse camber to enhance the stability of the aircraft during flight. The elevator is controlled using a fly-by-wire system, while the rudder is operated through a hydromechanical flight control system. Both the horizontal and vertical stabilizers are constructed using advanced composite materials, providing a lightweight and durable structure.

During the design process of the aircraft's tail unit, a conventional vertical tail configuration was chosen. The vertical tail, also known as the vertical stabilizer, serves

a vital role in maintaining balance, stability, and control over the aircraft's heading. It functions similarly to a flat tail design but is positioned only on the upper part of the aircraft axis. This arrangement accounts for the upward tilt of the aircraft's nose during take-off and landing, which brings the tail in close proximity to the ground, making it impractical to have a complete vertical tail surface.

Similar to a flat tail, the front half of the vertical tail surface remains fixed and is referred to as the vertical stabilizer. The rear half is hinged at the back of the stabilizer, allowing for steering and deflection, and is known as the rudder. The vertical tail fulfills multiple purposes, including maintaining a coordinated turn without side slip, aligning the aircraft's nose with the runway during crosswind landings, and counterbalancing the asymmetric yaw moment during flight, such as the yaw induced by the shutdown of one engine in a multi-engine configuration.

To mitigate yaw-related phenomena at high altitudes and speeds, a damper can be integrated into the rudder control system. The aircraft typically features a single vertical tail, known as a single vertical stabilizer, positioned within the plane of symmetry. This configuration ensures the aircraft's stability and control throughout various flight conditions.

Landing gear

Without this part of the aircraft, there can be no safe flights. Thanks to this component, not only take-off is ensured, but also a soft landing and easier taxiing. The landing gear is not just wheels, it is a whole mechanism of various devices.

Of the most important components of the landing gear, we need to remember about the shock absorbers, which help to make a smooth landing and about the wheels of the aircraft. These components are not all components, but they are also directly responsible for the movement on the ground.

After analyzing the prototype and reviewing previous years' inquiries, the decision was made to utilize the first three-point landing gear. This choice was based on several reasons.

The first three-point landing gear offers simplicity, safety, and reliability. When landing at speeds exceeding the specified value, the impact force on the main wheel

reduces the angle of attack sharply upon ground contact, eliminating the "jump" phenomenon associated with rear-front three-point landing gear. This type of landing gear provides excellent directional stability, ensuring safer landings in crosswind conditions. It also allows for more maneuverability and flexibility when taxiing on the ground. Strong braking is permitted without the risk of tipping over, which helps reduce the taxiing distance after landing. Furthermore, the aircraft's horizontal or nearly horizontal fuselage position during stop, take-off, and landing improves the downward field of view.

Although the first three-point type has its limitations, such as the complexity of arranging the nose landing gear, especially for single-engine aircraft, and the restricted space in the front of the fuselage, it still offers advantages. The nose landing gear bears a significant load, has a large size, and features a complex structure, resulting in increased mass. Additionally, the low angle of attack during landing roll limits the use of air resistance for braking. Overcoming obstacles on uneven runways may pose challenges, and there is a potential for shimmy in the front wheel, necessitating preventive measures and equipment, which adds complexity and weight to the front wheel.

However, given the high landing speeds of modern aircraft, prioritizing landing safety becomes the primary determining factor when selecting the landing gear type. In this regard, the first three-point configuration has clear advantages over the last three-point type, making it the most widely applied option.

Control system

After analyzing the control system of the "A320neo" prototype, it was determined that the cockpit of the aircraft designed includes two pilot seats: one for the captain and the other for the deputy captain. The flight control system comprises various components, including control surfaces, cockpit controls, hinges, and necessary mechanical mechanisms, which collectively regulate the aircraft's flight. The cockpit control devices are primarily as follows:

To manipulate the roll and pitch of the aircraft, control rods or cranks are securely connected to cylinders, allowing for the control of ailerons and elevators. The

yaw of the aircraft is controlled through rudder pedals. While certain aircraft may employ different forms of control surfaces like rudders or flaperons, the design prioritizes the use of control sticks for roll and pitch control and pedals for yaw control to prevent pilot confusion. In addition to the primary control devices for roll, pitch, and yaw, pilots may utilize auxiliary control devices to enhance flight control and reduce workload. One commonly used device is a wheel-shaped control for pitch and trim adjustments, which alleviates the pilot's effort in maintaining the aircraft's pitch balance. (Rudder trim and roll trim are typically found in larger airplanes, but some smaller airplanes may also be equipped with such features.) Many aircraft also incorporate lift-increasing devices, such as flaps, which facilitate take-off and landing. Additionally, the landing gear of certain aircraft can be retracted to modify the aircraft's air resistance. Advanced equipment, including intake flaps (which can increase drag and cool the engine), leading-edge slats, spoilers, and others, may also be present, each requiring corresponding operating equipment.

Crew cabin

The aircraft cabin encompasses the area designated for crew members, passengers, and luggage storage. It also accommodates essential equipment and emergency resources necessary for the duration of the flight. With a focus on passenger satisfaction and convenience, my aircraft design emphasizes an increased proportion of cabin space. Whether it is the economy class or business class, when designing passenger seating arrangements, prioritize widening the seats and aisle, ensuring ease of boarding, disembarking, and passage through the cabin. By enhancing passengers' overall experience and satisfaction, the aircraft can distinguish itself in the competitive landscape of modern civil aviation and establish its position as an innovative contender.

Passenger furnishing

Taking into consideration the passenger experience and comfort was a key aspect during the design of this aircraft, drawing from an analysis of the prototype aircraft and previous design cases. To enhance passenger convenience, kitchens were strategically placed at both ends of the cabin. These spacious areas were designed to accommodate the number of passengers on board, ensuring efficient food distribution and enhancing

overall passenger satisfaction. Furthermore, the inclusion of four toilets, each with a one-square-meter area, offers passengers convenient facilities for their personal use. Notably, the toilets are equipped with filter water tanks to facilitate hand and face washing, along with easily accessible toilet tanks for efficient flushing.

In terms of seating, the passenger seats were made adjustable. Specific inquiries were made regarding the prototype seat data to increase the seat distance. As a result, the distance between the front and rear seats has also been expanded, allowing passengers to adjust their seating according to their individual preferences. Additionally, the aircraft is equipped with three first aid kits, located in the front, middle, and rear compartments. This placement ensures easy access for passengers during emergency situations. Furthermore, essential safety features, including oxygen masks, fire extinguishers, and smoke masks, are provided throughout the aircraft. These safety facilities undergo regular inspections and maintenance by dedicated personnel. To ensure passenger awareness during emergencies, highly visible evacuation lights and "EXIT" signs are strategically positioned, enabling passengers to easily locate exits and follow instructions from flight attendants in critical situations.

Airborne equipment

The A320neo aircraft is equipped with a comprehensive range of airborne equipment necessary for its operation. This includes flight instruments, communication systems, navigation devices, environmental control systems, life support systems, and energy supply systems. Additionally, specific equipment related to the aircraft's functionality, such as weapons and fire control systems for fighter aircraft or cabin life services for civil aircraft, may also be incorporated.

To enhance its performance, the A320neo incorporates advanced aircraft electronic systems, including the air data inertial system, which boasts robust anti-interference capabilities. This system consists of several components, such as the ADIRS backup navigation system, landing navigation equipment system, relevant positioning system, and independent positioning system. Together, these systems ensure accurate and reliable navigation and positioning for the aircraft.

In addition to the essential airborne equipment mentioned above, the A320neo incorporates several innovative features that enhance its overall performance and passenger experience. One notable addition is the advanced fly-by-wire control system, which replaces traditional mechanical linkages with electronic signals. This system provides precise control inputs, improves maneuverability, and enhances the aircraft's efficiency. Furthermore, the A320neo features state-of-the-art avionics, including advanced cockpit displays and integrated systems. These advancements offer pilots enhanced situational awareness, streamlined information management, and efficient decision-making capabilities. The integration of modern avionics contributes to safer and more efficient flight operations. Moreover, the A320neo places a strong emphasis on fuel efficiency and environmental sustainability. It incorporates lightweight materials, aerodynamic improvements, and advanced engine technology to reduce fuel consumption and carbon emissions. These features not only benefit the environment but also result in cost savings for airlines.

Overall, the A320neo stands as a testament to the continuous advancement in aircraft design and technology. It combines cutting-edge airborne equipment, advanced electronic systems, and a commitment to fuel efficiency, making it a reliable and eco-friendly choice for airlines and a comfortable and enjoyable experience for passengers.

Power plant

The Pratt & Whitney PW1000G engine is one of the key components of the designed aircraft. It possesses significant thrust power, which amounts to 120 [kN]. The aircraft is equipped with two of these engines, providing it with additional strength and high-speed capabilities.

One of the important features of the PW1000G engine is its high bypass ratio of 12.5:1. This means that a substantial portion of the incoming air bypasses the core engine, resulting in reduced fuel consumption, lower noise levels, and improved environmental performance.

The PW1000G engine is designed using advanced technologies and materials, ensuring its efficiency and reliability. Its innovative construction allows for weight reduction while delivering optimal performance in various flight conditions.

Thanks to its characteristics, the Pratt & Whitney PW1000G engine is an attractive choice for aircraft design, aiming to enhance thrust, efficiency, and environmental sustainability. Its high thrust, twin-engine configuration, and optimal bypass ratio contribute to reliability and high performance during flights of different distances and conditions.

The specifications and performance characteristics of this engine can be found in Table 1.2.

Table 1.2

Examples of application engine

Engine Model	Overall Length [mm]	Overall Width [mm]	Dry Spec. Weight [kg]	Maximum Take-off Power		Normal Take-off Power		Maximum Continuous Power	
				Shaft Power [kW]	Max. Air Temp for Rated Power [°C]	Shaft Power [kW]	Max. Air Temp for Rated Power [°C]	Shaft Power [kW]	Max. Air Temp for Rated Power [°C]
PW1100G	3350	1880	3370	27000	32	24000	32	23000	40

Conclusions to the analytical part

In this part of the diploma project, it was supposed to develop a sketch project of a medium-haul aircraft capable of carrying 185 passengers. The creation of this aircraft was facilitated by the study of famous aircraft, namely the Airbus A320neo, COMAC C919, Airbus A320 and adding them to the desired prototypes. Thanks to the provided initial data, which were obtained with the help of modern computer programs, it was possible to execute these tasks.

The aircrafts design of the prototypes focuses on optimizing various aspects of its performance, passenger comfort, and safety. The wing configuration plays a crucial role in generating lift during flight, while mechanisms and additional components enhance take-off and landing characteristics. The fuselage, constructed with lightweight materials and employing a semi-monocoque design, ensures structural integrity and efficient load transfer. The tail unit, featuring stabilizers, elevators, and a rudder, contributes to the aircraft's balance, stability, and control. The landing gear system provides essential support for safe take-offs, landings, and ground maneuverability.

The control system incorporates cockpit controls and control surfaces, enabling pilots to manage the aircraft's flight movements effectively.

Selected engine Pratt & Whitney PW1000G, with its significant thrust power, high bypass ratio, advanced construction, and twin-engine configuration, is a crucial component of the designed aircraft, providing enhanced strength, efficiency, and environmental performance for flights of varying distances and conditions.

Additionally, the prototypes incorporates advanced airborne equipment and electronic systems.

2. MAIN PARTS OF THE AIRCRAFT CALCULATIONS

The layout is the arrangement of structures and parts of the aircraft. Also, these are all types of cargo, such as passengers, cargo, fuel etc.

The selection of the scheme, parameters and composition of the aircraft is necessary for optimal compliance with the requirements in operation.

2.1 Wing geometry calculation

In a special computer program, the data for the designed aircraft were calculated. The source data can be found in Appendix A.

Determine the wing area based on the weight m_0 and specific wing load P_0.

Wing area (S_{wing}):

$$S_{wing} = \frac{m_0 \cdot g}{P_0},$$

where: m_o – take off mass of the aircraft, g – gravitational acceleration, P_o – wing loading at cruise regime of flight.

$$S_{wing} = \frac{99035 \cdot 9.8}{5.432} = 178.671 \text{ [m}^2\text{]},$$

So, we take the wing area S_{wing} = 178.671 [m^2] .

Wing span is:

$$l = \sqrt{S_{wing} \cdot \lambda_w};$$

$$l = \sqrt{178.671 \cdot 9.4} = 40.98 \text{ [m]},$$

where: λ_w – aspect ratio of the wing.

Root chord is:

$$C_{root} = \frac{2S_w \cdot \eta_w}{(1+\eta_w) \cdot L};$$

$$C_{root} = \frac{2 \cdot 178.671 \cdot 3.98}{(1+3.98) \cdot 40.98} = 6.73 \text{ [m]},$$

where: η_w – efficiency factor of the wing.

Tip chord is:

$$C_{tip} = \frac{C_{root}}{\eta_w};$$

$$C_{tip} = \frac{6.73}{3.98} = 1.97 \text{ [m]};$$

On board chord for trapezoidal shaped wing is:

$$C_{board} = C_{root} \cdot \left(\frac{1-(\eta_w - 1) \cdot D_f}{\eta_w \cdot L_w} \right);$$

$$C_{board} = 8.39 \cdot \left(1 - \frac{(3.98-1) \cdot 5.64}{3.98 \cdot 48} \right) = 6.243 \text{ [m]},$$

where: D_f – diameter of the fuselage.

Wing construction and spars position.

The torsion box type with two spars was chosen. Relative coordination of the spar's position is equal for a wing with two spars: $x_{1spar} = 0.2$ C_i; $x_{2spar} = 0.6$ C_i from the leading edge of current chord in the wing cross-section.

The mean aerodynamic chord (MAC) of a wing is determined by geometric method. The geometrical method of mean aerodynamic chord determination has been taken, which is presented at the fig. 2.1.

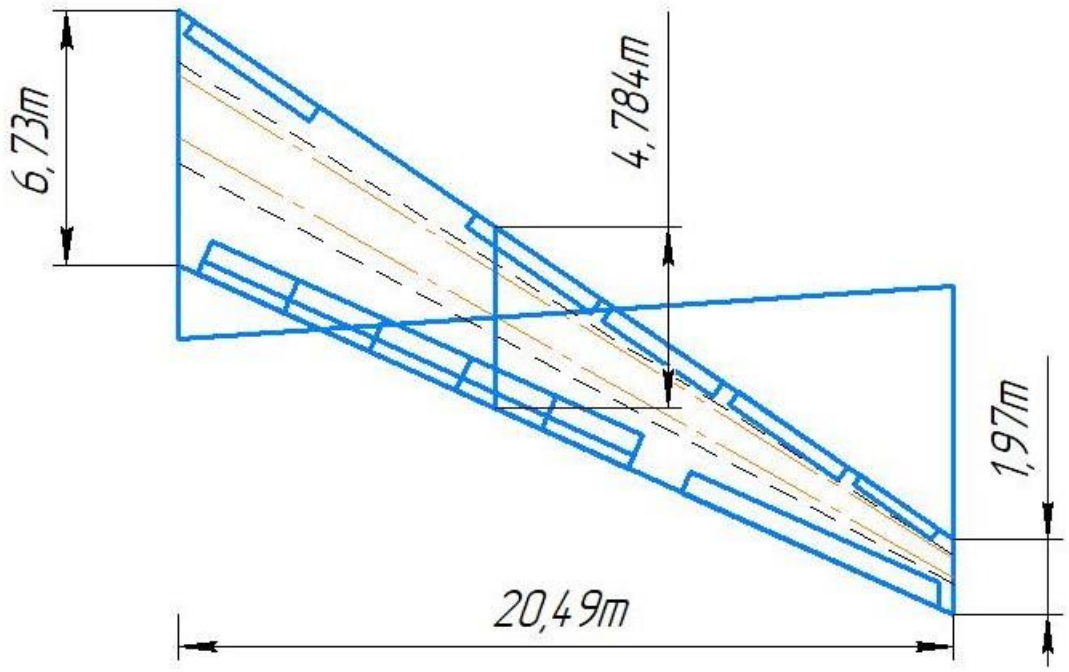

Figure 2.1 – Determination of mean aerodynamic chord.

Mean aerodynamic chord is equal $b_{MAC} = 4.784$ m.

We can also calculate the MAC of the wing using this formula:

$$b_{MAC} = \frac{2}{3}\frac{C_{root}^2 + C_{root}C_{tip} + C_{tip}^2}{C_{root} + C_{tip}};$$

$$b_{MAC} = \frac{2}{3}\cdot\frac{6.73^2 + 6.73\cdot 1.97 + 1.97^2}{6.73 + 1.92} = 4.784 \text{ [m]};$$

Once the geometric characteristics of the wing are established, the next step is to focus on the wing's mechanization and calculate the geometric properties of the

ailerons. This stage is crucial in optimizing the wing's functionality and maneuverability. By carefully considering the dimensions, shape, and positioning of the ailerons, engineers can ensure effective control of the aircraft along its longitudinal axis.

Ailerons geometrical parameters is equal to:

Ailerons span: $l_{aileron} = 0.35\frac{l_w}{2}$;

$$l_{aileron} = 0.35 \cdot \frac{40.98}{2} = 7.17 \text{ [m]};$$

Aileron area: $S_{aileron} = 0.06\frac{S_w}{2}$;

$$S_{aileron} = 0.06 \cdot \frac{178.671}{2} = 5.36 \text{ [m]};$$

Area of aileron’s trim tabs for two engines airplane:

$$S_{trim\ tabs} = (0.04 \ldots 0.06) S_{ail};$$

$$S_{trim\ tabs} = 0.04 \cdot 4.466 = 0.178 \text{ [m}^2\text{]};$$

Range of aileron deflection: upward $\delta_{aileron} \geq 25^{\circ}$ downward $\delta_{aileron} \geq 15^{\circ}$;
High lift device of a wing: Double slotted flaps combined with slats.
Aerodynamic compensation of the aileron:

Axial: $S_{axinail} \leq (0.25 \ldots 0.28) S_{ail} = 0.28 \cdot 5.36 = 1.5 \text{ [m}^2\text{]}.$

2.2 Fuselage layout

The layout of the fuselage is the correct placement of cargo and passengers in the aircraft. The shape of the skin is given by frames and bulkhead. The spars are interconnected in parallel with formers across the entire surface. At the beginning of

the fuselage the first frame is the pressurized bulkhead, which provide the sealing for the cabin. At the rear part of the fuselage the aft pressure bulkhead is located before auxiliary power unit to close the pressurized cabin.

The fuselage of the aircraft consists of three parts: front, middle and rear. The front is the cockpit, the middle is the passenger compartment, the rear is the tail unit. An image of the layout of the aircraft can be seen in fig. 2.2.

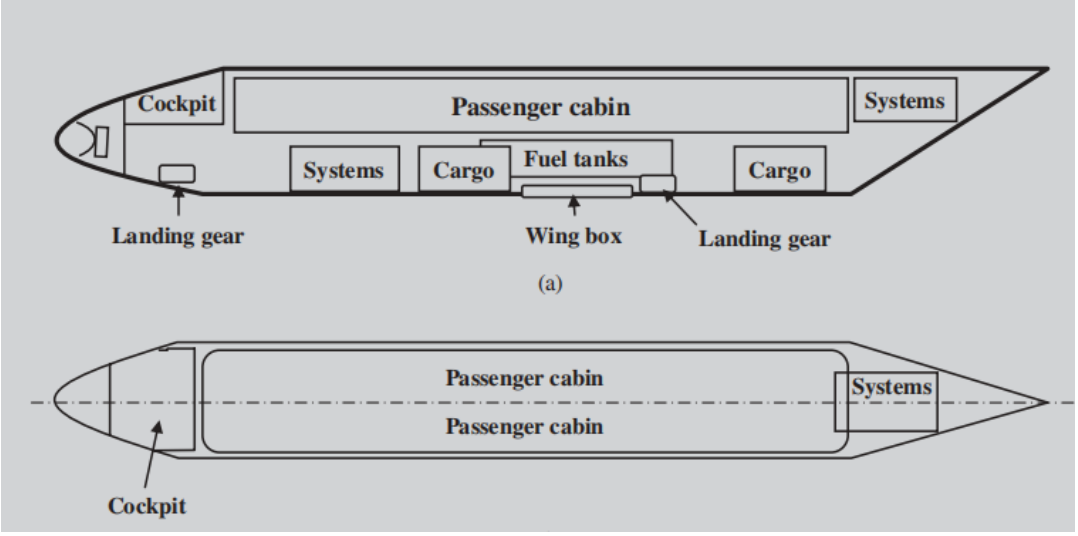

Figure 2.2 – Preliminary design of aircraft layout.

Length of the aircraft fuselage:

$$FR = \frac{L_{fus}}{D_{fus}};$$

$$L_{fus} = FR_f \cdot D_f;$$

$$L_{fus} = 9 \cdot 4.2 = 37.8 \text{ [m]},$$

where: FR – fineness ratio of the fuselage, D_{fus} – diameter of the fuselage.

Length of aircraft fuselage forward part:

Once the thickness coefficient of the forward fuselage is determined for the prototype, it serves as the baseline for further analysis and design considerations.

This coefficient is a crucial parameter that influences the structural integrity and aerodynamic performance of the aircraft.

$$L_{fwd} = FR_{np} \cdot D_{fus};$$

$$L_{fwd} = 1.4 \cdot 1.2 = 5.8 \text{ [m]};$$

Length of the fuselage tail part:

$$L_{tail\ pavt} = FR_{tu} \cdot D_{fus};$$

$$L_{tail\ part} = 1.6 \cdot 4.2 = 6.72 \text{ [m]};$$

Cabin width:

For the economy class cabin, passenger seats according to the 3 + 3 scheme in each row.

$$B_{cabin} = n_2 b_2 + n_3 b_3 + n_{aisle} + b_{aisle} + 2\delta + 2\delta_{wall};$$

$$B_{cabin} = 2 \cdot 1430 + 1 \cdot 400 + 2 \cdot 30 + 2 \cdot 80 = 3480 \text{ [mm]};$$

For the business class cabin, passenger seats according to the 2 + 2 scheme in each row.

$$B_{cabin} = n_2 b_2 + n_{aisle} + b_{aisle} + 2\delta + 2\delta_{wall};$$

$$B_{cabin} = 2 \cdot 1340 + 1 \cdot 500 + 2 \cdot 90 + 2 \cdot 100 = 3560 \text{ [mm]};$$

Cabin height:

$$H_{cabin} = 1.48 + 0.17 B_{cabin};$$

$$H_{cabin} = 1.48 + 0.17 \cdot 3.48 = 2.07 \text{ [m]};$$

Length of the cabin:

It is necessary to set the correct seat pitch relative to the class for the convenience of passengers.

Cabin length L_{cab} for typical accommodation with constant seat pitch L_{seat}:

$$L_{cab} = L_1 + (N-1)L_{seat} + L_2;$$

$$L_{cab} = 1200 + (33-1)\cdot 750 + 135 = 25335 \text{ [mm]},$$

where: L_1 – distance from the wall to the back of the seat in first row, mm, L_2 – distance from the back of the seat in the last row to the wall, mm.

The length of economic passenger cabin:

$$L_{econ} = L_1 + (N-1)L_{seatpitch} + L_2;$$

$$L_{econ} = 1200 + (28-1)\cdot 750 + 235 = 21685 \text{[mm]};$$

The length of business passenger cabin is equal to:

$$L_{busi} = L_1 + (N-1)L_{seatpitch} + L_2;$$

$$L_{busi} = 1200 + (5-1)\cdot 900 + 235 = 5035 \text{ [mm]};$$

Baggage compartment

The correct placement of luggage on an aircraft is crucial for maintaining the aircraft's center of gravity. Accurate calculations are necessary to determine the optimal positioning of cargo and impose weight restrictions. Mishandling the placement of luggage can have severe consequences during flight, potentially leading to accidents and compromising the safety of the aircraft and its occupants.

The unit of load on floor K = 400… 600 kg/m^2

The area of cargo compartment is defined:

$$S_{cargo} = \frac{M_{bag}}{0.4K} + \frac{M_{cargo\&mail}}{0.6K};$$

$$S_{cargo} = \frac{20 \cdot 185}{0.4 \cdot 600} + \frac{15 \cdot 185}{0.6 \cdot 600} = 23.1 \text{ [m}^2\text{]},$$

where: M_{bag} – mass of baggages of all passengers, $M_{bag} = m\ n_{pass}$, m – mass of baggage for one passenger for free, n_{pass} – number of passengers, $M_{cargo\ \&mail}$ – mass of additional cargo and mails on the board of aircraft.

Cargo compartment volume is:

$$V_{cargo} = \nu \cdot n_{pass}\ ;$$

$$V_{cargo} = 0.2 \cdot 185 = 37\ \text{[m}^3\text{]};$$

Luggage compartment design is similar to the prototype.

The design of the luggage compartment bears resemblance to that of the prototype, showcasing similarities in their configurations and layout.

Galleys and buffets:

International standards provide for food, dishes, depending on the duration of the flight and depending on the layout of the aircraft. If the flight lasts less than 3 hours, then meals are not provided, but it is possible to get water or tea. Buffets and toilets can be left on the flight for less than an hour.

$$V_{galley} = 0.1 \cdot n_{pass};$$

$$V_{galley} = 0.1 \cdot 185 = 18.5\,[\text{m}^3];$$

The total area of galley floor:

$$S_{galley} = \frac{V_{galley}}{H_{cab}};$$

$$S_{galley} = \frac{18.5}{2.07} = 8.93[\text{m}^2];$$

Lavatories:

$$t = \frac{R_{flight}}{V_{cruise}} + 0.5;$$

$$t = \frac{5700}{870} + 0.5 = 7.05\,[\text{h}];$$

$$N_{lavatory} = \frac{N_{pass}}{40};$$

$$N_{lavatory} = \frac{185}{40} > 4$$

The number of lavatories is determined according to the original airplane.

Area of lavatory:

$$S_{lavatory} = 1.5\,[\text{m}^2];$$

Width of lavatory: 1m. The design of the toilets exhibits similarities to that of the prototype, showcasing resemblances in their overall layout and features.

On aircraft, 2 galleys and 4 lavatories are designed.

2.3 Layout and calculation of basic parameters of tail unit

The position of the tail unit (TU) is one of the most crucial decisions made during the aerodynamic layout. It directly affects the aircraft's stability, control, and overall performance.

The range of the static moment coefficient for the horizontal tail unit A_{htu} and the vertical tail unit A_{vtu} is determined based on statistical data. Typical arm lengths are provided for the horizontal tail unit HTU and the vertical tail unit VTU relative to the mean aerodynamic chord of the wing. These values help ensure proper balance and stability of the aircraft.

$$S_{HTU} = (0.18 \ldots 0.25) S;$$

$$S_{HTU} = 0.25 \cdot 178.671 = 44.66 \ [\text{m}^2];$$

$$S_{VTU} = (0.12 \ldots 0.20) S;$$

$$S_{VTU} = 0.2 \cdot 178.671 = 35.73 \ [\text{m}^2];$$

In the first approach count that $L_{HTU} \approx L_{VTU}$ and find it from the dependences:

Trapezoidal scheme, normal scheme:

$$L_{VTU} = (0.2 \ldots 3.5) b_{MAC};$$

$$L_{VTU} = 2.2 \cdot 4.784 = 10.52 \ [\text{m}];$$

Determination of the elevator area and direction:

Elevator area:

$$S_{el} = (0.3 \ldots 0.4) S_{HTU};$$

$$S_{el} = 0.3 \cdot 44.66 = 13.39 \ [\text{m}^2];$$

Rudder area:

$$S_{rudder} = (0.2 \ldots 0.22) S_{VTU};$$

$$S_{rudder} = 0.2 \cdot 35.73 = 7.146 \ [\text{m}^2];$$

Choose the area of aerodynamic balance.

$$0.3 \le M \le 0.6;$$

$$S_{ab\ el} = (0.22 \ldots 0.25) S_{el};$$

$$S_{ab\ el} = 0.22 \cdot 13.398 = 2.94\,[\text{m}^2];$$

$$S_{ab\ \text{rudder}} = (0.2 \ldots 0.22) S_{rudder};$$

$$S_{ab\ \text{rudder}} = 0.22 \cdot 7.146 = 1.43\,[\text{m}^2];$$

If the speed of the flight $M \ge 0.75$, than:

$$S_{ab\ el} \approx S_{ab\ rudder} = (0.18 \ldots 0.2) S_{control\ surfase};$$

$$S_{ab\ el} \approx S_{ab\ rudder} = 0.18 \cdot 10.3 = 1.85\,[\text{m}^2];$$

The area of trim tab:

$$S_{tabs} = (0.8 \ldots 0.12) S_{rudder};$$

$$S_{tabs} = 0.8 \cdot 7.146 = 5.71\,[\text{m}^2];$$

Determination of the TU span.

TU span is related to the following dependence:

$$l_{HTU} = (0.32 \ldots 0.5) l_{wing};$$

$$l_{HTU} = 0.32 \cdot 40.98 = 13.11\ [\text{m}];$$

In this dependence the lower limit corresponds to the turbo jet engine aircraft, equipped with all-moving stabilization.

The height of the vertical TU h_{vtu} is determined accordingly to the location of the engines. Taking it into account:

Low wing, EonW, M < 1

$$h_{VTU} = (0.14 \ldots 0.2) l_{wing};$$

$$h_{VTU} = 0.14 \cdot 40.98 = 5.73\,[\text{m}];$$

Tapper ratio of horizontal and vertical TU we need to choose:

For planes M < 1 $\eta_{HTU} = 2.5,\ \eta_{HTU} = 1.25;$

For transonic planes $\lambda_{VTU} = 1,\ \Lambda_{HTU} = 3.5;$

Determination of TU chords b_{tip}, b_{MAC}, b_{root}:

$$b_{tip} = \frac{2S_{HTU}}{(\eta_{HTU} + 1) l_{HTU}};$$

$$b_{tip} = \frac{2 \cdot 44.66}{(2.5 + 1) \cdot 13.11} = 1.94\ [\text{m}];$$

$$b_{MAC} = 0.66 \cdot \frac{\eta_{HTU}^2 + \eta_{HTU} + 1}{\eta_n + 1} \cdot b_{HTU\ tip};$$

$$b_{MAC} = 0.66 \cdot \frac{2^2 + 2.5 + 1}{2.5 + 1} \cdot 1.94 = 2.74\ [\text{m}];$$

$$b_{root} = b_{tip} \cdot \eta_{HTU};$$

$$b_{root} = 1.94 \cdot 2.5 = 4.85\ [\text{m}];$$

TU sweptback is taken in the range 3...5˚, and not more than wing sweptback. It is necessary to provide the control of the airplane in shock stall on the wing.

2.4 Calculation of basic parameters and layout of landing gear

At this stage, when the drawing is still missing, only a part of the landing gear parameters can be determined (fig. 2.3).

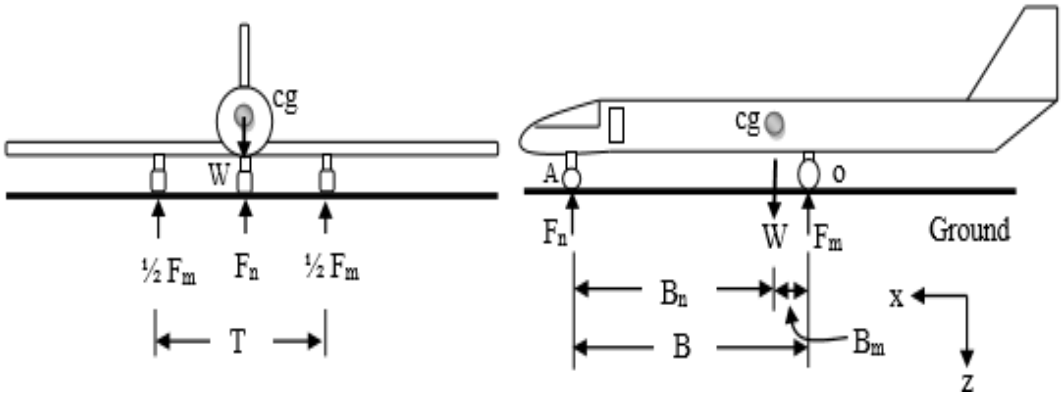

Figure 2.3 – The distance from the centre of gravity to the main LG.

Main wheel axes offset is:

$$B_m = k_e \cdot b_{MAC};$$

$$B_m = 0.2 \cdot 4.784 = 0.95 \text{ [m]};$$

where: k_e – coefficient of axes offset $\left(k_e = 0.15 \ldots 0.3\right)$;

Landing gear wheel base comes from the expression:

$$B = k_b = \left(0.3 \ldots 0.4\right) \cdot l_f = (6...10) B_m;$$

$$B = 0.3 \cdot 37.8 = 10 \cdot 0.95 \text{ [m]};$$

$$11.34 > 9.568;$$

where: k_b – wheel base calculation coefficient.

$$B_n = B - B_m;$$

$$B_n = 11.34 - 0.95 = 10.38 \text{ [m]};$$

Wheel track is:

$$T = k_T = (0.7 \ldots 0.12) B \leq 12;$$

$$T = 0.7 \cdot 11.34 = 7.93 \text{ [m]};$$

where: k_T – wheel track calculation coefficient.

Wheel track is the distance between the outer wheels of the main gear. Wheels for the landing gear is chosen by the size and run loading on it from the take off weight; for the front support consider dynamic loading also.

The load on the wheel is determined by the formula:

$$\sum F_z = 0 \rightarrow F_n + F_m = W$$
$$\sum M_0 = 0 \rightarrow F_n B + W B_m = 0$$

$$F_n = \frac{B_m}{B} W$$

$$F_n = \frac{B_n}{B} W$$

Static load on main:

$$F_{main} = \frac{(B - B_m) m_0 \cdot 9.81}{B \cdot n \cdot z};$$

$$F_{main} = \frac{(11.34 - 0.95) \cdot 99035 \cdot 9.81}{11.34 \cdot 2 \cdot 2} = 222390 \text{ [N]};$$

Nose wheel load is:

$$F_{nose} = \frac{B_m \cdot m_0 \cdot 9.81 \cdot k_g}{B \cdot z};$$

$$F_{nose} = \frac{0.95 \cdot 99035 \cdot 9.81 \cdot 1.5}{11.34 \cdot 2} = 61579 \text{ [N]};$$

$$n = 2, z = 2,$$

where n, and z – is the quantity of the supports and wheels on the one leg.

$k_g = 1.5...2.0$ – dynamics coefficient.

By calculated F_{main} and F_{nose} and the value of $V_{take\ off}$ and $V_{landing,}$ pneumatics is chosen from the catalog, the following correlations should correspond.

$$P^K_{sl\ main} \geq P_{main}; P^K_{sl\ nose} \geq P_{nose}; V^K_{landing} \geq V_{landing}; V^K_{takeoff} \geq V_{takeoff};$$

Pressure in the wheel pneumatics should range in $P = (3\ldots5)10^5$, [Pa].

It is crucial to adhere to this specified pressure range to ensure proper functioning and performance of the aircraft's wheels.

The selection of tires for an aircraft is a crucial consideration that depends on the maximum load exerted on the wheels during take-off and landing. To make an informed decision, it is beneficial to reference prototypes and their specific characteristics [3]. For further guidance, Table 2.1 provides a comprehensive overview of the selected tires.

Additionally, to visualize the main landing gear configuration of the Airbus A320neo, refer to fig. 2.4. These visual representations aid in understanding the physical components involved in the aircraft's landing gear system.

Figure 2.4 – Main landing gear of Airbus A320neo.

Table 2.1

Nose gear

Size	Construction			Service Rating				Tread Design/ Trademark	Weight [Lbs]
	Ply Rating	TT or TL	Rated Speed [mph]	Rated load [Lbs]	Rated Inflation [Psi]	Max. Breaking Load [Lbs]	Max. Bottoming Load [Lbs]		
H29× 9.0-15	16	TL	210	14.500	196	21750	39200	Flight Leader	43.9

Inflated Dimensions [in]				Static Loaded Radius [in]	Aspect Ratio	Wheel [in]			
Outside DIA		Section Width				Width Between Flanges	Specified Rim Diameter	Flange Height	Min Ledge Width
Max	Min	Max	Min						
29	28.2	9	8.5	12.3	0.777	6	15	0.95	2.15

Table 2.2

Main gear

Size	Construction			Service Rating				Tread Design/ Trademark	Weight [Lbs]
	Ply Rating	TT or TL	Rated Speed [mph]	Rated load [Lbs]	Rated Inflation [Psi]	Max. Breaking Load [Lbs]	Max. Bottoming Load [Lbs]		
49×17	32	TL	235	50.40	210	72600	151200	Flight Leader	223.0

Inflated Dimensions [in]				Static Loaded Radius [in]	Aspect Ratio	Wheel [in]			
Outside DIA		Section Width				Width Between Flanges	Specified Rim Diameter	Flange Height	Min Ledge Width
Max	Min	Max	Min						
48.75	47.7	17.25	16.4	20.2	0.839	13.25	20	1.88	3.65

The rate of wheel loading is:

for nose wheel:

$$\frac{14500 - 13843.51}{14500} \cdot 100 = 4.52\ [\%];$$

for main wheel:

$$\frac{50400 - 49995.29}{50400} \cdot 100 = 0.8\ [\%];$$

The selected tires for this airplane can be utilized since their values are below 10%.

2.5 Center of gravity calculation

Trim-sheet of the equipped wing

Many factors affect the center of gravity on board, not only mass, but shifting mass will change the center of gravity. During flight, the center of gravity of an aircraft will always change due to fuel consumption. In order to calculate the center of gravity, first need to find the displacement of the mass. To do this, it is necessary to divide the mass into two parts: the mass of the wing with equipment and the mass of the fuselage with equipment.

The total weight of the equipped wing is influenced by various factors, such as the fuel quality, construction quality, landing gear, and equipment integrated within the wing. Coordinates of the center of gravity for the equipped wing are defined by the formula:

$$X_w^{/} = \frac{\Sigma m_i^{/} x_i^{/}}{\Sigma m_i^{/}}$$

All wing masses of the designed aircraft are presented in Table 2.1.

Table 2.1

Trim-sheet of equipped wing

N	Object name	Mass		C.G coordinates Xi, [m]	Mass moment, Xi × m(i)
		Units	Total mass m(i), [kg]		
1	Wing (structure)	0.11359	11249.38565	2.05712	23141.33621
2	Fuel system	0.0096	950.736	2.0332	1933.036435
3	Flight control system, 30%	0.00168	166.3788	2.8704	477.5737075
4	Electrical equipment, 10%	0.00315	311.96025	0.4784	149.2417836
5	Anti-ice system, 65%	0.00868	859.6238	0.4784	411.2440259
6	Hydraulic systems, 70%	0.01113	1102.25955	2.8704	3163.925812
7	Power plant	0.09818	9723.2563	-1.6	-15557.21008
8	Equipped wing without landing gear and fuel	0.24601	24363.60035	0.563100186	13719.14789
9	Nose landing gear	0.0055	544.6925	-11.38	-6198.60065
10	Main landing gear	0.0316	3129.506	0.6	1877.7036
11	Fuel	0.32214	31903.1349	2	63806.2698
	Total	0.60525	59940.93375	1.221277616	73204.52064

Trim-sheet of the equipped fuselage

The CG coordinates of the FEF are determined by the formula:

$$X_f = \frac{\Sigma m_i^{/} X_i^{/}}{\Sigma m_i^{/}};$$

After it determined the C.G. of fully equipped wing and fuselage, we construct the moment equilibrium equation relatively to the fuselage nose:

$$m_f x_f + m_w (x_{MAC} + x_w^{/}) = m_0 (x_{MAC} + C);$$

where: C – distance from MAC leading edge to the C.G. point, determined by the designer.

$$C = (0.22...0.25)\, B_{MAC},$$

$$C = 0.25 \cdot 4.784 = 1.196;$$

Table 2.2

Trim-sheet of equipped fuselage

N	Objects names	Mass		C.G coordinates Xi, [m]	Mass moment
		Units	Total mass		
1	Fuselage	0.06829	6763.10	18.9	127822.59
2	Horizontal tail	0.00873	864.57	9.56	8272.25
3	Vertical tail	0.00866	857.64	10.52	9026.52
4	Radar	0.003	297.10	1	297.10
5	Radio equipment	0.0022	217.87	1	217.87
6	Instrument panel	0.0052	514.98	2	1029.96
7	Aero navigation equipment	0.0045	445.65	2	891.31
8	Flight control system 70%	0.0039	386.23	18.9	7299.86
9	Hydraulic system 30%	0.00477	472.39	26.46	12499.62

10	Electrical equipment 90%	0.02835	2807.64	18.9	53064.43
11	Not typical equipment	0.0032	316.91	3	950.73
12	Lining and insulation	0.0064	633.82	18.9	11979.27
13	Anti ice system, 35%	0.00434	429.81	30.24	12997.51
14	Airconditioning system	0.008680	859.62	18,9	16246.88
15	Passenger seats (bussiness)	0.001158483	114.73	5.92	679.77
16	Passenger seats (economic class)	0.01216407	1204.66	20	24093.37
17	Seats of flight attendence	0.000289621	28.68	1.82	52.2
18	Seats of pilot	0.000241351	23.90	1.48	35.37
19	Emergency equipment	0.001246476	123.44	8.1	999.9
20	Lavatory1, galley 1	0.0065	643.72	2.96	1905.43
21	Lavatory2, galley 2	0.0065	643.72	30	19311.82
22	Operational items	0.01887	1868.79	26	48588.55
23	Additional eguipment	0.00321	317.90	5	1589.51
24	Equipped fuselage without payload	0.2104	20836.96	17.26	359851.93
25	Passengers (economy)	0.130969859	12970.6	20	259412
26	Passengers (bussiness)	0.009330035	924	5.92	5474.7
27	On board meal	0.002362801	234	30	7020
28	Baggage	0.031504014	3120	18	56160
29	Cargo, mail	0.006967234	690	18	12420
30	Flight attend	0.002423386	240	17	4080
31	Crew	0.001555006	154	2.4	369.6
	TOTAL	0.39551234	39169.56	17.99	704788.23
	TOTAL fraction for checking	1.000762335	99110.49		

Calculation of center of gravity positioning variants

The list of mass objects for centre of gravity variant calculation given in Table 2.3 and Center of gravity calculation options given in Table 2.4, completes on the base of both previous tables.

Table 2.3

Calculation of C.G. positioning variants

N	Name	Mass in kg	Coordinate	Mass moment
1	Object	m_i	X_i, [m]	[kgm]
2	Equipped wing (without fuel and landing gear)	24363.6	16.95	412941.22
3	Nose landing gear (extended)	544.69	5.00	2723.46
4	Main landing gear (extended)	3129.51	17.00	53201.60
5	Fuel reserve	3517.31	18.39	64669.37
6	Fuel for flight	30386.03	18.39	558677.71
7	Equipped fuselage (without payload)	20836.96	17.27	359851.93
8	Passengers (economy)	12970.6	20.00	259412
9	Passengers (bussiness)	924	5.93	5474.70
10	On board meal	234	30.00	7020
11	Baggage	3120	18.00	56160
12	Cargo, mail	690	18.00	12420
13	Flight attend	240	17.00	4080
14	Crew	154	2.40	369.60
15	Nose landing gear (retrected)	544.69	4	2178.77
16	Main landing gear (retrected)	3129.51	17.86	55892.98

Table 2.4

Airplanes C.G. position variants

N	Name object	Маса, m_i [кГ]	Mass moment m_iX_i	center of mass $X_{цм}$
1	Take off mass (L.G. extended)	99035	1797001.6	17.77
2	Take off mass (L.G. retracted)	99035	1799148.28	17.79
3	Landing weight (LG extended)	70724.68	1238323.88	17.5
4	Ferry version (without payload, max fuel, LG retracted)	82932.11	1454581.58	17.53
5	Parking version (without payload, without fuel foe flight, LG extended)	52392.08	893387.58	17.05

Conclusions to the project part

In the project part considerable attention was paid to the calculation and analysis of the main components that make up the aircraft structure. This included a comprehensive assessment of the fuselage, tail section, wings and landing gear. In order to meet the given requirements, careful calculations were made.

Due to the desire to achieve optimal design, efficiency and passenger comfort, a comprehensive analysis of the factors affecting these criteria was carried out.

Comprehension of the complex interaction between aircraft components in the design process based on prototype aircraft provided valuable practical experience.

When calculating the design of the aircraft, it is worth knowing the center of mass of the aircraft for its safe operation in the future. The position of the center of mass of the aircraft directly affects the stability and controllability in flight and taxiing stability on the ground, so it is necessary to ensure that the center of gravity is always in the correct range. This is an important stage in the aircraft design process, because the center of mass determines exactly where the weight of the aircraft is concentrated and how it is distributed along its length, width and height. The calculation determines the optimal load distribution to ensure an even distribution of weight between the various components, including passengers, cargo and fuel. This affects the preservation of flight stability and efficiency.

3. NANOTECHNOLOGIES AGAINST ICING

3.1 Introduction to the special part

Ice buildup on aircraft is a major trouble. Ice forms on the wing and can be several centimeters thick [4]. Even thin ice on critical parts of an aircraft is dangerous when it reduces lift of the aircraft's ability and throw drag, which can lead for enhancing the functioning of the engine problems. There are two main methods of managing wing ice: anti-icing (avoiding ice buildup) and the action of de-icing (removing ice once it forms). Most technologies focus on deicing and assume that ice will form on the wings. Therefore, their goal is to remove the ice before it becomes a problem.

There are several options for countering aircraft icing. The A320neo is equipped with a number of features to help eliminate this problem: equipment designed to counteract icing, engine exhaust, ice detectors and wing surface protection. Ice detectors notify the crew of problems using sensors that provide information to activate the equipment for countering icing. Exhaust air from the engines also prevents icing as hot compressed air can be directed onto the outer wing sections. The wings are also protected by heating panels and, of course, have a special coating on the surface. That is, hot air anti-icing systems are based on the principle of supplying heated air to the wing surface, which prevents the formation of ice and removes existing ice. The key element of the air-thermal the system dedicated to ice prevention is special openings in the wings of the aircraft via where the heated-up air is supplied. This heated air is directed to the surface of the wings where it effectively prevents inhibit the formation of ice and promotes soften any ice that does form. As a result, the system provides trustworthy safeguarding against icing, which is a key factor in flight safety. Of course, the wind thermal an anti-icing system features a number of advantages that make it the best choice for flight safety:

- Effectiveness: the system provides dependable anti-icing safeguarding by preventing the freezing of aircraft wing areas and minimizing ice accretion. This assists in:
- Maintain optimal aerodynamic capabilities and provides stability and control during flight.
- Reliability: air heating systems are a reliable solution proven by operational lifespan and experience in the aviation industry. The system provides steadfast and unwavering protection against icing, which is very vital for the safety and comfort of passengers.
- Automation: the system has automatic control and adjustment functions without frequent crew intervention, which ensures its efficient operation. This allows the pilot to concentrate on other aspects of flying and controlling the aircraft.

Of course, all this helps to eliminate the problem, but it still requires some effort and has its drawbacks:

- Engine dependency: the air heating system entailshot air from the aircraft engine. If there is an engine problem or the wings need to be warmed up during a ground stop, the system may be unavailable or limited.
- Limited efficiency at high speeds: at high speeds, the efficiency of the air heating system may be limited. This occurs due to intensive heat dissipation from high wind speeds, which reduces the system's ability to inhibit ice buildup.
- Energy and fuel costs: solutions for countering ice formation require additional energy and fuel to heat the air and deliver it to the wing surfaces. This leads to increased fuel consumption and operating costs.

Need for regular servicing and scrutiny: regular maintenance tasks, of course inspection, and replacement of components is necessary to ensure reliable operation of the apparatus for warming the air. This entails additional resources, time and costs to maintain the aircraft.

Limited efficiency in extreme prerequisites: systems that transfer heat from air can face limitations in extreme weather conditions, such as extremely cold

temperatures or dense snowfall. In such cases, additional measures may be required to ensure full protection against icing.

3.2 Nanoparticles

Nanoparticles are particles with a size in nanometers from 1 to 100 [5], which helps them exhibit various properties that distinguish them from other large materials. They get a lot of attention for many reasons. Their properties may differ from the main material. Even if this is not the case, the creation of materials in the form of nanoparticles (especially by solution methods) can be advantageous in situations where the synthesis of a bulk material is challenging, expensive or arduous. For instance, nanoparticles integrated into specific materials have been found to exhibit extremely strong catalytic and adsorption properties. Other materials with excellent optical properties include the ultrathin films of organic matter utilized to make solar cells. Despite the lower quantum efficiency, these cells are cheaper and mechanically flexible. It has been established that artificial nanoparticles can interact with natural nanoscale objects such as proteins, nucleic acids, etc. Carefully purified nanoparticles have the ability to self-organize into specific structures. This structure contains strictly ordered nanoparticles. In addition, they often show unusual properties.

Due to its scientific and practical applications in many fields, such as nanodefects, electronics, and functional coatings, nanoparticle thin film is becoming increasingly popular, regardless of the reason for creating nanoparticles. Synthesis has a number of technologies and methods. Evaporation, deposition, mechanical fabrication methods and chemical synthesis.

Chemical synthesis is a common method of creating nanoparticles. It comes from chemical reactions that produce substances that are mixed together and then reacted to produce the desired results. Chemical synthesis of nanoparticles can involve the use of solutions, emulsions, gels, and other chemical media to create different types of particles. In this procedure, the size and morphology of those nanoparticles are changed by changing the reaction parameters such as temperature, solvent, components and concentration.

Mechanical processing is one of the oldest methods of creating nanoparticles. This procedure involves the reduction of larger materials into smaller ones by fragmentation, grinding, or slicing into particles. Nanoscale particles of the desired size and shape can be produced by various mechanical processes such as grinding, or vibration.

Another method of obtaining nanoparticles is evaporation, this method is based on the physical process of evaporation of a substance. In this procedure, a substance, usually a metal or compound, is heated to a very elevated temperature to vaporize it. Atoms or molecules that evaporate then aggregate and form nanoparticles. This technique is employed to create metal nanoparticles and nanofilms.

In order to produce nanoparticles, there are industrial enterprises, universities and specialized scientific laboratories that are controlled for production. The size, chemical composition and specifications of the nanoparticle formation process can be adjusted using high-tech equipment.

Discussions about the use of nano-sized particles have been going on for a long time in various proportions. Aircraft maintenance, inspection and non-destructive testing costs are only focused on bad forecasts. Currently, there are various methods of finding problems in the plane in addition to visual inspection, including shirography, ultrasonic control, and others [6]. In addition to the length and complexity of these procedures, they require full integration, but they do the job of finding damage and acting on that damage assessment. At the same time, nanoparticles are attractive because they are durable and do not require strict control and constant costs.

Due to their small size, lightness, and stability, as well as unique traits, on account of high electrical conductivity, they have the potential for revolutionary applications in the aerospace industry [7]. Their integration with existing composites, coatings and electronics can bring many benefits and bring aircraft efficiency and functionality taking things to an unprecedented level.

Using nanomaterials in aircraft could open up many possibilities. They will allow reducing the weight of the aircraft, giving it great strength and resistance to the effects of disasters and natural events. In addition, the introduction of nanomaterials

can create intelligent control and monitoring systems inside the aircraft to ensure the safety of passengers and the efficient operation of the aircraft.

As funding and innovation in nanomaterials and aerospace technology increases, it can expect the use of nanomaterials in aircraft to become more widespread, with applications in all aspects of design, safety systems, and aerodynamics. This will open up new vistas for the development of modern aviation and point the way to a future in which aircraft become more efficient, safer and more resistant to external influences.

There are diverse nanoparticles that can be interviewed in the skin of the wing. Silver nanofilm is an excellent conductor of electric current, and a way to cheaply produce this kind of film has already been found. It is very flexible its conductive material is silver nanowires (fig. 3.1). They are made by spraying particles on a wire through tiny nozzles at supersonic speeds. As a result, the conductivity of the film is approximately proportional to the conductivity of silver. What is important is that the shape of the surface does not matter. It can be both three-dimensional objects and plastic film.

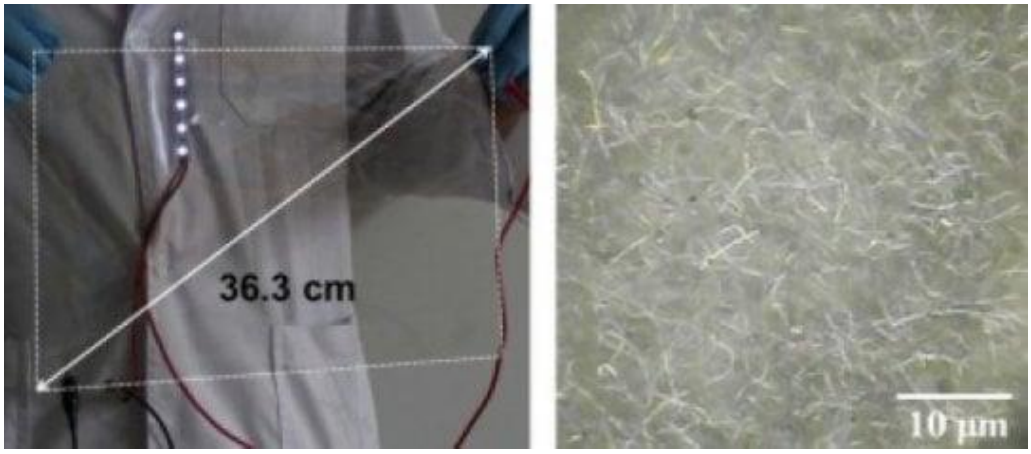

Figure 3.1 – Silver nanowire particles.

There are so-called hybrid nanocomposites, which differ from ordinary composites in terms of mechanical strength and heat transfer. There are multiple methods available for obtaining these materials. A distinction is made between the embedding of polymers and nanoparticles in layered architectures and the sol-gel

approach. Langmuir-Blodgett films that already contain nanoparticles consisting of metal elements are a promising material for nanocomposite fabrication. This hybrid nanocomposite exhibits conductive properties only in non-boundary component to polymer ratios when conductive channels from metal-containing clusters appear in the polymer matrix.

The most discussed conductive heating material is graphite-based thin film. Two types of expanded graphite are utilized for the fabrication of heating membranes: ABG 1010 and ABG 1045. PVA (Sigma Aldrich – 70,000-100,000 MW) based heating membranes were prepared using dispersive sonication.

A 60/40 exfoliated graphite/PVA mass ratio was chosen for both graphites (fig. 3.2) [8]. This specific composition makes it possible to obtain molded flexible foils based on graphite. This aspect is relevant because some parts of the aircraft are more vulnerable than others.

In-flight icing occurs most often on the leading edge of an aircraft's wing, typically covering only 2% of the wing chord length. For both graphites, a mass ratio of expanded graphite/PVA equal to 60/40 was chosen, and this composition allowed to obtain molded flexible foils based on graphite, the flexibility of this film allowed it to be used also in curved geometries.

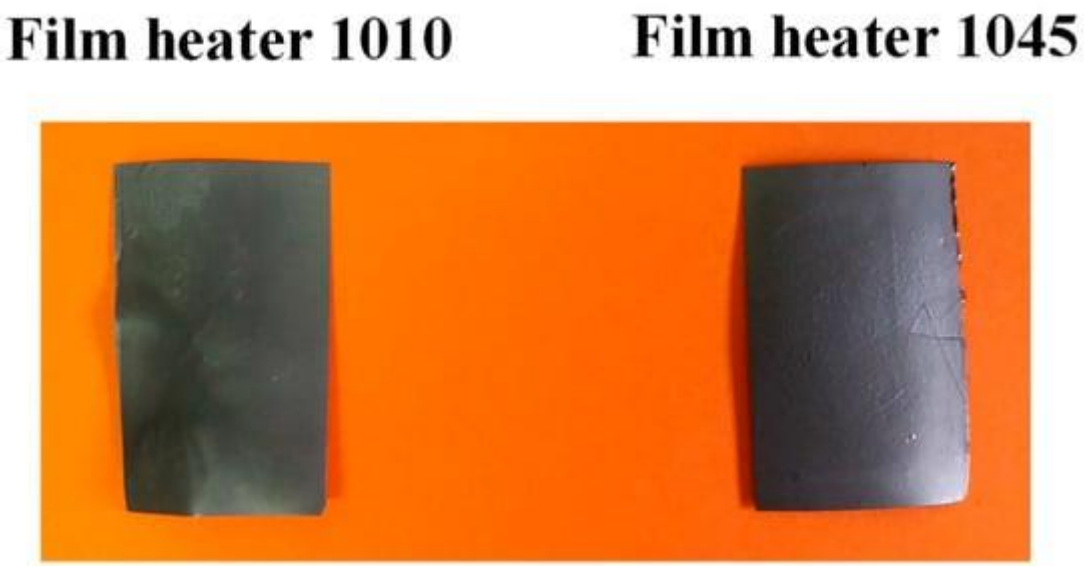

Figure 3.2 – Optical images of film heaters.

If nanomaterials become conductive at filler concentration values above the electrical threshold, they can be heated using the Joule effect. The heat released is related to the current flow in the conductive polymer nanomaterial, and some energy is lost due to lattice oscillations [9]. As a result of the flow causing the release of heat, heat is generated, and a segment of the heat is lost due to the the vibration of the crystal lattice phonons. Electrons can be scattered with the involvement of phonons, ionized impurities, vacancies, and electron-electrons as they migrate with the assistance of the device under the influence of an electric field. The process of electron-impurity scattering is not accompanied via the energy conversion from the electron in the direction of the lattice due to large mass of impurities compared to the mass of the electron. In addition, electron-electron scattering does not affect the lattice temperature; therefore, the only scattering mechanisms are electron-phonon scattering mechanisms.

The so-called carbon nanotubes [10] can be described as tubular-shaped constructs with a specific diameter of having diameters in the nanometer range and lengths of ranging spanning from a few micrometers up to plenty of inches. Separately "carbon nanotube" is molded via either one or multiple graphene planes that have been rolled into a tube.

An enlarged view of this nanotube is shown in the image below (fig. 3.3). The nanotube has a significantly improved appearance in the image, which allows it to study its structural features in more detail. Through magnification techniques, the complex characteristics of a nanotube become more apparent. This allows for a closer study and evaluation of its unique design and properties.

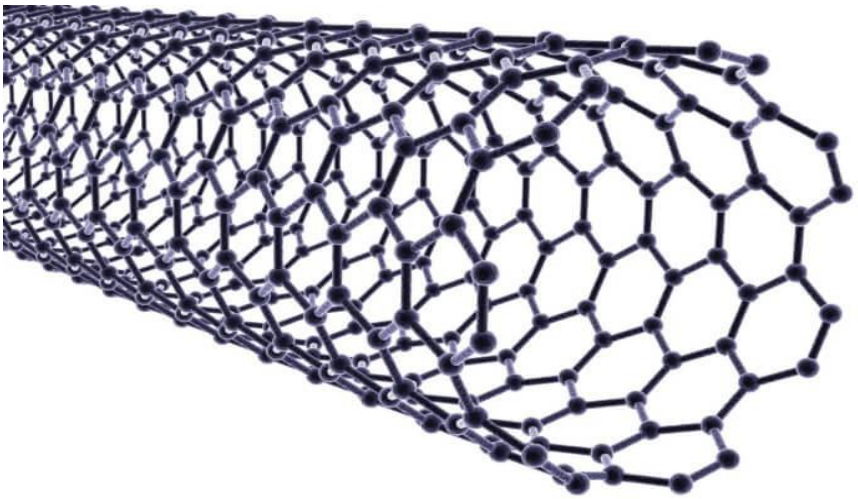

Figure 3.3 – Nanotubes.

Their physical attributes of the nanotubes directly depend on their chirality. Chirality is determined with the help of special indicators (n, m), which reflect the ratio of the dimensions and the angle of narrowing of the tube (α) (fig. 3.4). These parameters determine the shape and structure of the nanotube. Chiral nanotubes differ from achiral ones in that their mirror image does not coincide with the tubes themselves. This means that nanotubes have unique geometries and can have a variety of physical properties. This dependence between chirality and characteristics of nanotubes opens wide opportunities for understanding their behavior and application in various fields of science and technology.

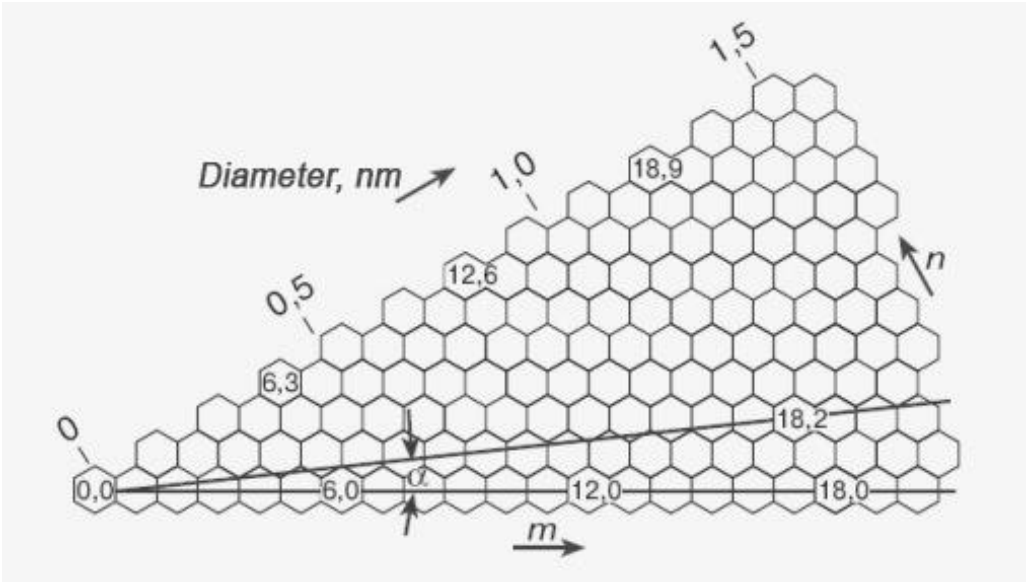

Figure 3.4 – Size and alignment of the tube's axis.

The size and alignment of the tube's axis in relation with respect to the graphene plane are governed by the indices indicating chirality (n, m), which are representations the placements that determine radius vector R within a two-dimensional plane inclined the spatial reference system. The hexagon grid should be located where the hexagonal pattern originating at the origin is due to the fusion process of the tube, as shown by these indices.

A carbon nanotube is a kind of pattern from a graphene layer, and just as can see in the image above, it is given by two numbers (n, m). In order to calculate the diameter of a nanotube, use knowledge about the diameter of the cylinder. The circumference of this cylinder must be equal to the value of the vector R (its length).

The previously mentioned chirality indices (n, m) help with this:

$$D = \frac{\sqrt{3} d_0}{\pi} \cdot \sqrt{n^2 + m^2 + nm};$$

where $d_0 = 0{,}142$ [nm] - the distance between adjacent carbon atoms in the graphite plane.

Exist a connection between the chirality values (n, m) and it also keeps it between the angle α, which gives the ratio:

$$\sin a = \frac{m\sqrt{3}}{2\sqrt{n^2 + m^3 + nm}};$$

Now, by understanding what nanoparticles look like, what they are and where they are used, can select exactly what will help improve the properties of an aircraft wing. Now it can often hear about nanofilms based on graphite or carbon. They really have properties that are not inherent in all nanocomposites. A nanofilm based on carbon nanotubes is a good option for heating the wing skin according to the already discussed Joule heating principle. They conduct heat perfectly, thereby allowing current to be directed through them.

When current penetrates the nanofilm, the nanotubes create Joule heating [11], converting electrical energy into thermal energy. Thus, the temperature of the

nanotubes becomes higher, which in turn increases the degree of heat of the wing skin in which they would hypothetically be integrated.

Thus, the carbon nanotube-based nanofilm, functioning as an electrically conductive element, can generate heat and heat the skin of an aircraft wing, helping to prevent the formation and reduce the accumulation of icing.

This nanofilm based on carbon nanotubes can be located between the components of the composite material of aircraft wings and, due to the large percentage of nanoparticles and their corresponding electrical conductivity, can be used for anti-icing. This is an effective method not only to fight against the buildup of a large layer of ice (both on the leading edges of the wing and on its entire area), but also an effective strategy in the fight against environmental pollution due to the reduction of high fuel consumption for heating the skin surface due to to prevent the formation of unwanted solid deposits.

With a decrease in the fuel spent on heating the skin, the weight of the aircraft will also decrease, as the exclusion of the anti-icing system in the wings of the aircraft will give free weight either for any implementations.

3.3 Calculation of aircraft weight and fuel efficiency

Thanks to nanoparticles, the plane can be lightened, providing the opportunity to reduce fuel consumption compared to an aircraft equipped with an anti-icing system. If necessary, excess fuel can be eliminated, leading to a decrease in the weight of the aircraft and potential alternative utilization. This includes extending the flight time of the aircraft, enabling longer journeys over extended distances. However, the objective remains to calculate fuel efficiency, and utilizing this formula will help determine the required value by determining fuel consumption:

$$a = \frac{2 \cdot R_0 \cdot m_{empty}}{m_0 \cdot m \cdot V_c};$$

where: R_0 – thrust-to-weight ratio, m_{empty} – empty aircraft weight, m_0 – take-off weight, m – commercial payload, V_c – cruise speed.

For calculation fuel consumption according to this formula, we need to know the unknown value V_C. To calculate the V_C value, we can substitute the corresponding values taken from the original aircraft data, which were calculated based on the prototype aircraft:

$$V_p = V_{cs} \cdot \frac{L}{L + 0.16 \cdot V_{cs} + 160};$$

where L – flight range.

To begin with, we will convert the cruise speed from [km/h] to [m/s] and flight range kilometers [km] to meters [m]:

$$V_{cs} = 870 \text{ [km/h]} \rightarrow 241.56 \text{ [m/s]};$$

$$L = 5700 \text{ [km]} \rightarrow 5700000 \text{ [m]};$$

Now substitute values:

$$V_p = 241.56 \cdot \frac{5700000}{5700000 \cdot 0.16 \cdot 241.56 + 160} = 241.55 \text{ [m/s]};$$

Based on the calculation and initial data, we get the result:

$$a = \frac{2 \cdot 2.3 \cdot 52392.08}{99035 \cdot 19332.5 \cdot 241.55} = 5.21 \times 10^{-7} \text{ [1/(kgs)]}.$$

Now the fuel efficiency of the plane is known. In order to calculate it after the anti-icing system is replaced by nanofilms, it is necessary to find out what the empty weight of the aircraft will be without the anti-icing system.

According to the Table 2.1, we can consider the mass of individual elements of the wing and select the necessary numbers for calculation.

To begin with, it is necessary to add the anti-icing mass in the wing to the anti-icing mass of the fuselage.

$$G_{anti\ ice} = F_{anti\ ice} + W_{anti\ ice},$$

$$G_{anti\ ice} = 859.62 + 429.81 = 1289.43\ [\text{kg}];$$

where $F_{anti\ ice}$ – anti-icing mass in the fuselage, $W_{anti\ ice}$ – anti-icing mass in the wing.

The next step is to subtract the total weight of the anti-icing system from the empty weight of the aircraft. Where is this value M_{wais} – the mass of the object excluding the presence of an anti-icing system:

$$M_{wais} = 52392.08 - 1289.43 = 51102.65\ [\text{kg}];$$

Now that all the necessary values are known, it is possible to calculate the fuel efficiency when all anti-icing systems are turned off from the aircraft:

$$a = \frac{2 \cdot 2.3 \cdot 51102.65}{99035 \cdot 19332.5 \cdot 241.55} = 5.08 \times 10^{-7}\ [1/(\text{kgs})].$$

The aircraft can be lightened, providing the opportunity to reduce fuel consumption compared to an aircraft equipped with an anti-icing system. If necessary, excess fuel can be eliminated, leading to a decrease in the weight of the aircraft and potential alternative utilization. This includes extending the flight time of the aircraft, enabling longer journeys over extended distances. Based on the results of the calculations, you can follow how the fuel efficiency has changed and how much lighter the plane has become. This means that it has become more productive and cheaper to operate.

3.4 Wing skin with nanofilm

To obtain the desired to conduct electric current, it is necessary to distribute the electrically conductive nanoparticles over the entire volume of the solid material, as a result of which there will appear systems in matrices based on which the matrix is a polymer. After this action, this material becomes electrically conductive at a certain value of nanofiller. Its concentration must exceed a certain threshold of filtered electricity (percolation), due to which it becomes possible to heat the nanomaterial using the Joule effect [12]. This heat is a consequence of the electrical flow that passes through the nanomaterial. He also investigates the loss of energy subsequently to the lattice wave.

The polymers in the film will be elastomers. They have high elastic properties as well as viscosity. It is customary to call an elastomer any material that has elasticity and is able to stretch so many times that its length will exceed the initial one. Increasing the concentration of the graphite filler in the polymer matrix increases the heating power from 0.3 to 3.2 [kW/m^2]. Its temperature at a voltage of 100 watts can reach a temperature of 71.4 degrees Celsius. The modified elastomer with graphite material allows the heater to be produced in a variety of designs including through-hole designs which can be important when complex layouts are required.

This heater is a film heater and is made on the basis of graphite (fig. 3.5):

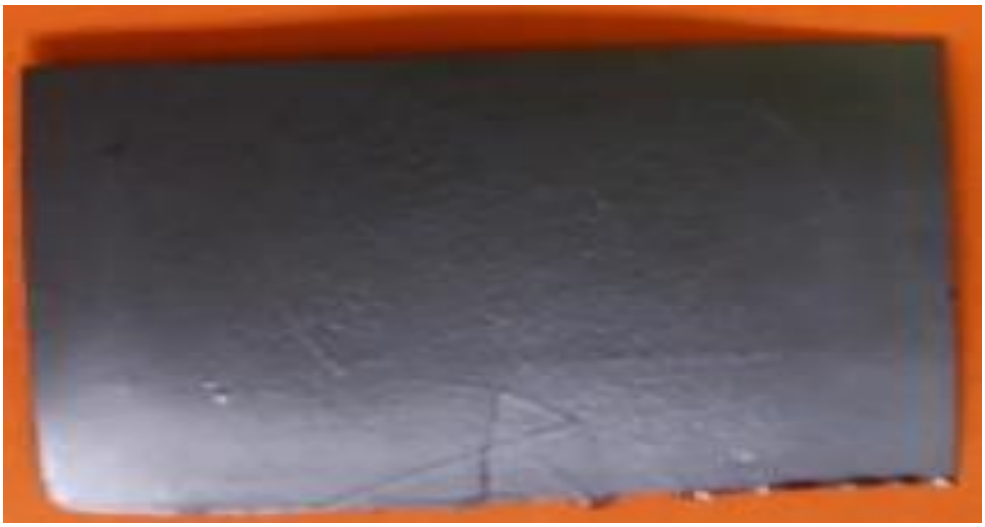

Figure 3.5 – Graphite film heater.

In order to visually illustrate the presence of the film in the wing, the 3D modeling software Catia V5 will be used. The wing design itself will be simplified, since the main task is to depict the presence of a film in the wing skin.

The nanofilm will be located directly in the wing skin, so first it was necessary to create a wing frame for a better illustration. In the image (fig. 3.6) there is an opportunity to see the wing stringers, spars, ribs and other components of the wing.

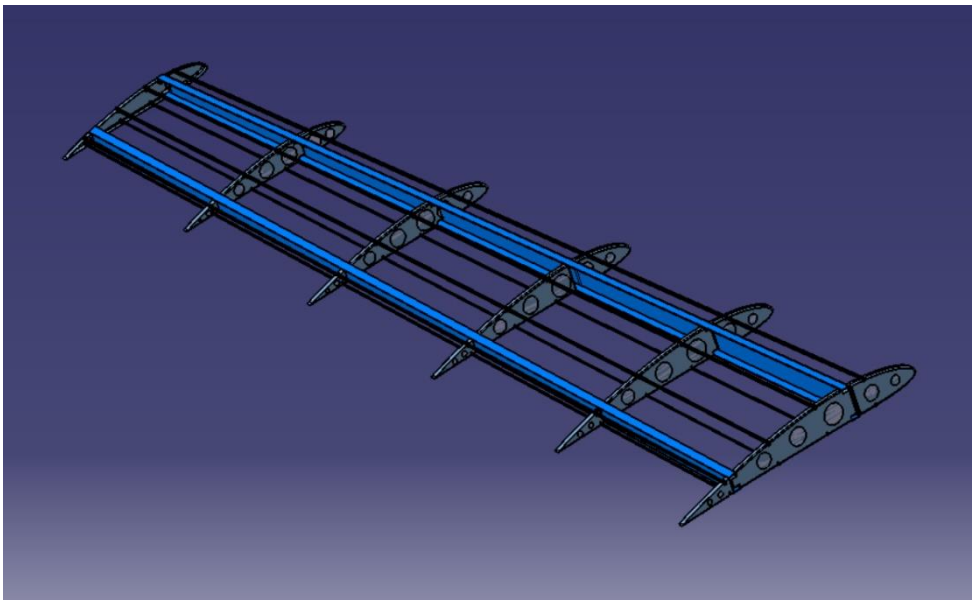

Figure 3.6 – Wing frame.

The presence of a 3D model of the main components of the wing frame makes it possible to sheathe the wing with a skin for further imaging of the nanofilm.

The following image (fig. 3.7) illustrates the wing skin.

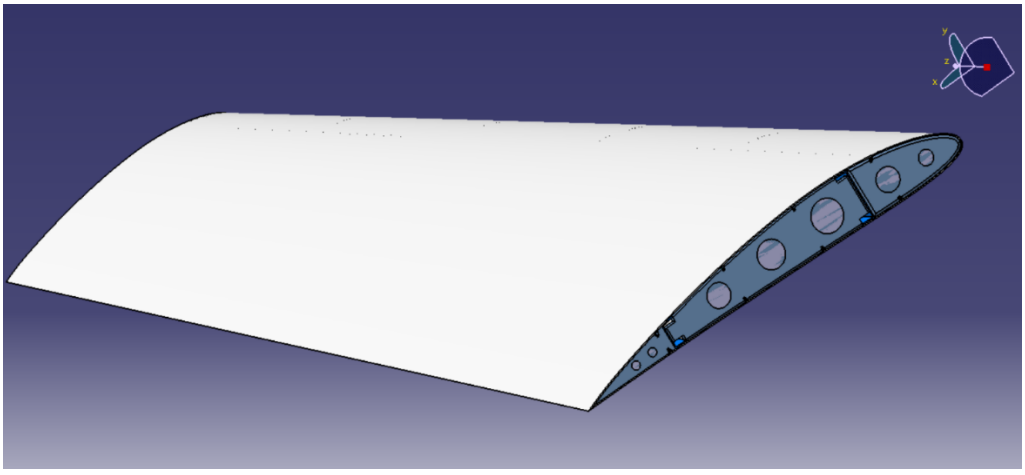

Figure 3.7 – Wing skin.

This nanofilm, as mentioned above, is located among the skin materials, that is, directly inside it. Due to its low weight, this will not negatively affect the wing skin in any way, but on the contrary, it will improve its quality due to its excellent electrical conductor properties.

In order to show the nanofilm, it is necessary to divide the skin layer into two parts. The film will lie on the bottom, it will also be covered by the second layer of skin. The figure (fig. 3.8) shows a small fraction of the nanofilm that lies on the first skin layer.

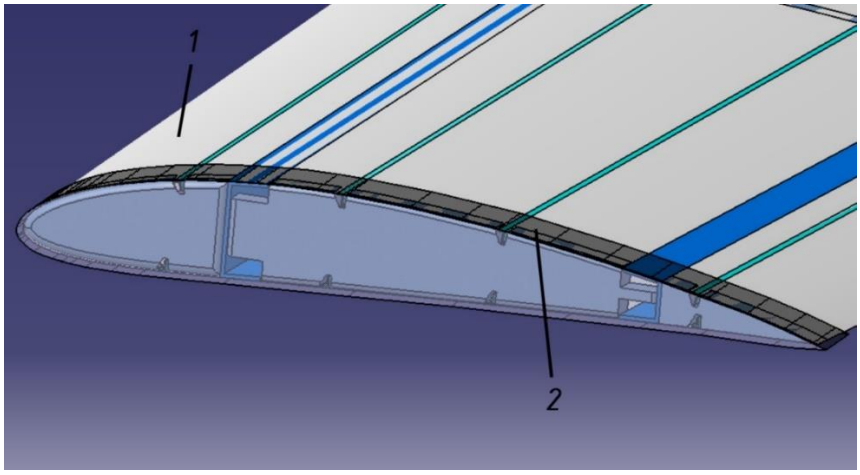

Figure 3.8 – The lower part of the skin with the underlying nanofilm:
1 – wing skin, 2 – nanofilm.

The overlapping of the film with the top layer of the skin is shown in the following image (fig 3.9).

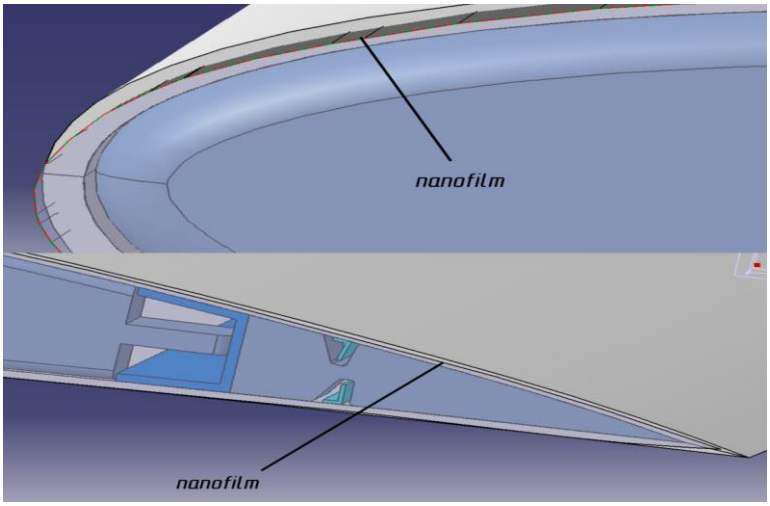

Figure 3.9 – The lower part of the skin with the underlying nanofilm.

Similar graphene heaters have also been tested inside various composite materials (fig. 3.10) [13].

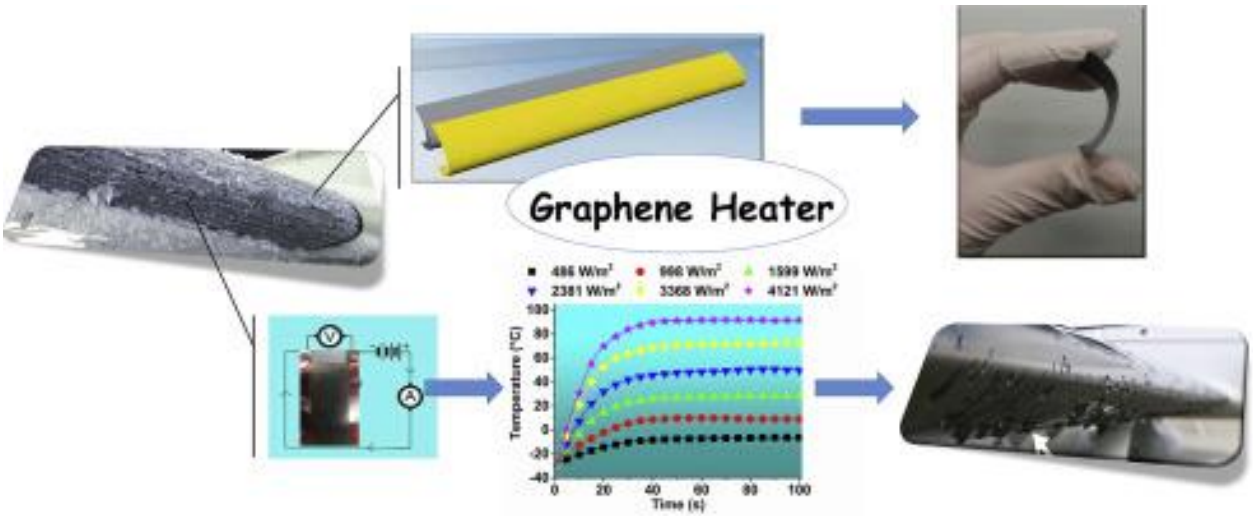

Figure 3.10 – Graphene heater.

The visual image of this coating without taking into account the wing skin can be seen by removing the top and bottom layers. This manipulation is carried out in the pictures fig. 3.11 – 3.12.

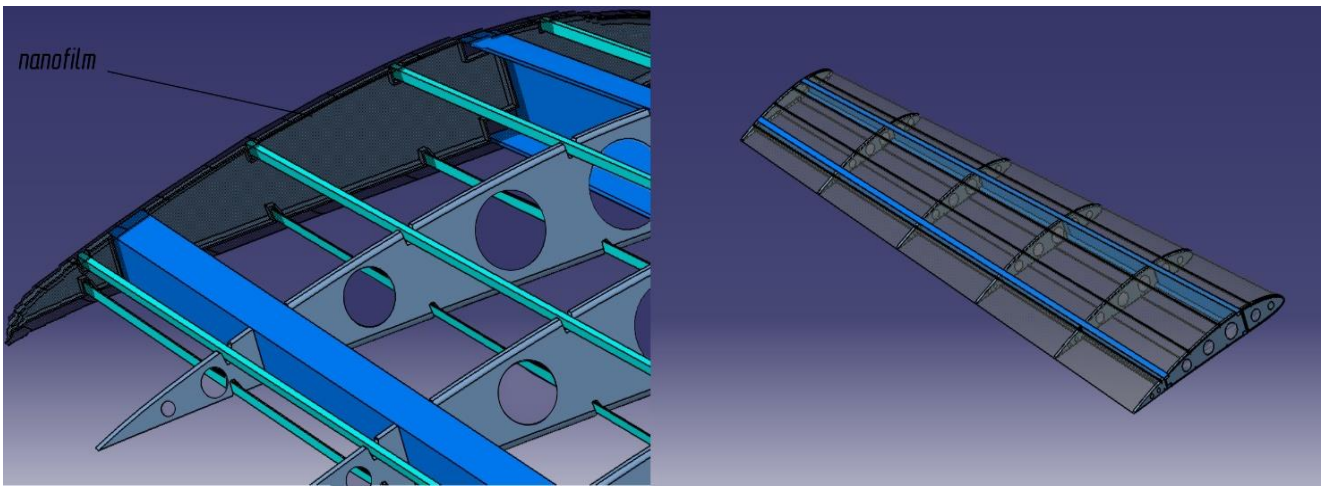

Figure 3.11 – Light coverage with nanofilm and full coverage.

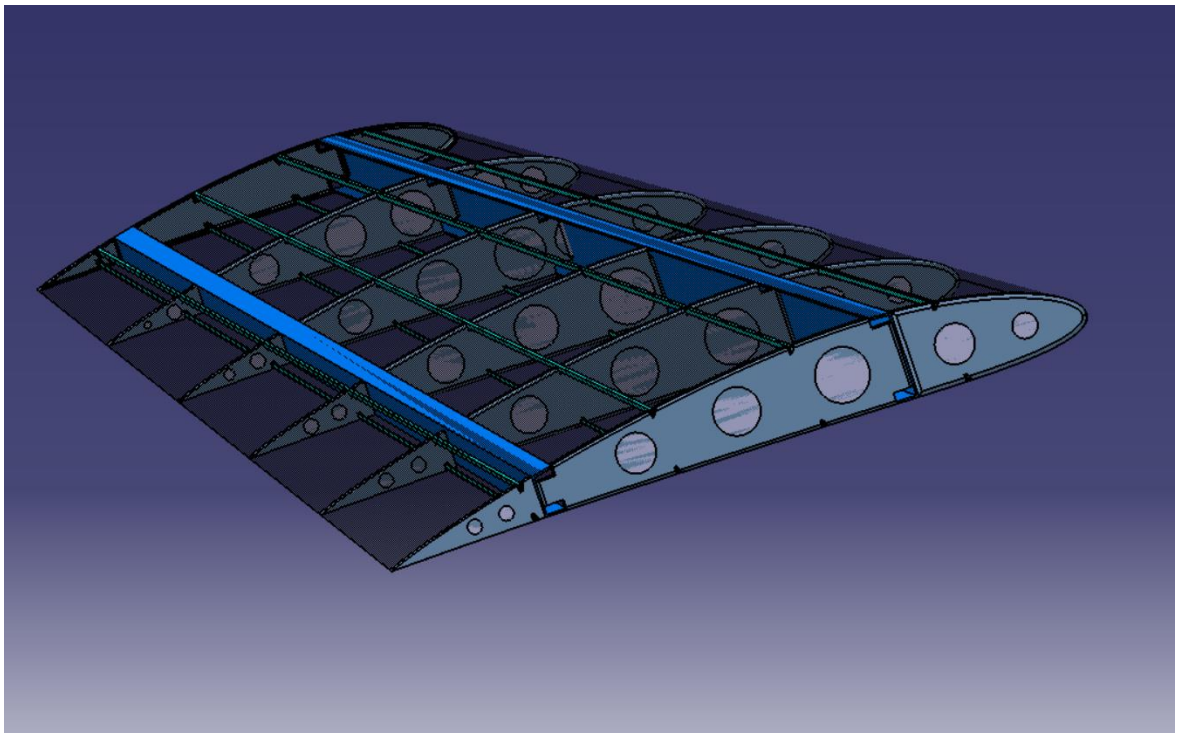

Figure 3.12 – Light coverage with nanofilm and full coverage.

Conclusions to the special part

In this special part of the qualification paper, the use of nanotechnologies for anti-icing was considered.

Despite the presence of anti-icing systems in prototype aircraft, they have their own shortcomings that they encounter during operation. Ranging from problems with ice sensors, ending with the requirement of constant checks and system failures.

Nanofilms based on carbon nanotubes have unique properties, which makes it possible to use them for heating the wing skin using Joule heating. The integration of these films between the layers of composite materials in the wing can provide a solution to all of the above problems from icing.

Their implementation is a promising strategy for icing, as well as reducing fuel consumption and its release into the environment.

GENERAL CONCLUSIONS

Conclusion, what was done during the writing of this thesis highlights some key points: Development of a draft design of a medium-haul aircraft, which was made based on three prototypes (Airbus A320neo, COMAC C919, Airbus A320), also with the help of which the initial data for further work. Aircraft design calculations and analyzes were carried out, which gave a practical understanding of aircraft design and components.

To achieve optimal load distribution, as well as control and stability of the aircraft, calculations of the center of mass were carried out. This is of no small importance in the aircraft design process, as the data that is obtained has implications for the stability, safety, flight efficiency and controllability of the pilot.

In a special part of the diploma project, the use of nanotechnology to improve the performance of the aircraft in the fight against icing was considered. Nanofilms based on carbon nanotubes have shown unique electrically conductive abilities. They can be integrated into the wing structure to solve many problems due to icing on the wing. This is especially important for the leading edge of the wing, since ice several centimeters wide grows there. This will eliminate problems due to malfunction, failures and many other negative factors of the anti-icing system.

The integration of new technologies for the continued safe operation of the aircraft is essential, as is the understanding of all aircraft design principles to improve various aspects of aviation. Therefore, it is important to find new technologies that can help extend the life of various components.

REFERENCES

1. Airbus A320neo [Electronic source] // Airliners Inform – Access mode URL: https://www.airlines-inform.com/commercial-aircraft/airbus-a320neo.html.
2. COMAC C919 the new Chinese airliner. [Electronic source] // Modern Airliners – Access mode URL: https://modernairliners.com/comac-c919/
3. Aircraft Tire Data Book – Akron: GoodYear, 2018. – 22 p.
4. Xingliang J. Studies on the Electro-Impulse De-Icing System of Aircraft / J. Xingliang, W. Yangyang. // MDPI. – 2019. – P. 1–2.
5. Mandal A. What are Nanoparticles? [Electronic source] / Ananya Mandal // News-medical. – 2019. – Access mode URL: https://www.news-medical.net/life-sciences/What-are-Nanoparticles.aspx.
6. Staszewski W. Health Monitoring of Aerospace Structures / W. Staszewski, C. Boller, G. Tomlinson. – Munich: Department of Mechanical Engineering, 2004. – 265 p. – (John Wiley & Sons).
7. Critchley L. The Potential for Nanotechnology in the Aerospace Industry [Electronic source] / Liam Critchley // Mouser electronics. – 2022. – Access mode URL: https://www.mouser.com/blog/potential-nanotechnology-aerospace-industry.
8. Low-Voltage Icing Protection Film for Automotive and Aeronautical Industries [Electronic source] / [L. Guadagno, F. Fabiana, P. Roberto et al.] // MDPI. – 2020. – Access mode URL: https://www.mdpi.com/2079-4991/10/7/1343.
9. Ragab T. Joule heating in single-walled carbon nanotubes / T. Ragab, C. Basaran. // Journal of applIied physics. – 2009. – V. 106.

10. Carbon nanotubes, their production, properties and applications [Electronic source] // Science Alpha. – 2019. – Access mode URL: https://sciencealpha.com/carbon-nanotubes-their-production-properties-and-applications/.
11. New Aircraft Anti/de-Icing Technologies / L.Vertuccio, F. Foglia, R. Pantani, L. Guadagno. // Materials Science and Engineering. – 2020. – №1757. – C. 6.
12. Joule-Heating Effect of Thin Films with Carbon-Based Nanomaterials / [U. Kiran, S. ORCID, D. Esteves et al.]. // MDPI. – 2022. – №1996. – P. 15.
13. Effective de-icing skin using graphene-based flexible heater [Electronic source] / [L. Vertuccio, F. De Santis, R. Pantani et al.] // ScienceDirect. – 2019. – Access mode URL: https://www.sciencedirect.com/science/article/pii/S1359836818321620#cebib0010.

Appendix

Appendix A

INITIAL DATA AND SELECTED PARAMETERS

Passenger Number 185.
Flight Crew Number 2.
Flight Attendant or Load Master Number 5.
Mass of Operational Items 1869.06 kg.
Payload Mass 19332.50 kg.

Cruising Speed 870 km/h.
Cruising Mach Number 0.8055.
Design Altitude 10.00 km.
Flight Range with Maximum Payload 5700 km.
Runway Length for the Base Aerodrome 2.95 km.

Engine Number 2.
Thrust-to-weight Ratio in N/kg 2.3000 N/kg.
Pressure Ratio 32.50.
Assumed Bypass Ratio 4.50.
Optimal Bypass Ratio 4.50.
Fuel-to-weight Ratio 0.2400.

Aspect Ratio 9.40.
Taper Ratio 3.40.
Mean Thickness Ratio 0.120.
Wing Sweepback at Quarter Chord 32.0 degree.
High-lift Device Coefficient 1.300.
Relative Area of Wing Extensions 0.050.
Wing Airfoil Type-supercritical.
Winglets-yes.
Spoilers-yes.
Fuselage Diameter 4.20 m.
Finess Ratio 9.00.
Horizontal Tail Sweep Angle 35.0 degree.
Vertical Tail Sweep Angle 40.0 degree.

CALCULATION RESULTS

Optimal Lift Coefficient in the Design Cruising Flight Point 0.45013.
Induce Drag Coefficient 0.00909

ESTIMATION OF THE COEFFICIENT D m = M critical - M cruise

Cruising Mach Number 0.80553.
Wave Drag Mach Number 0.81817.
Calculated Parameter D m 0.01265.

Wing Loading in kPa (for Gross Wing Area):
At Takeoff 6.521.
At Middle of Cruising Flight 5.432.
At the Beginning of Cruising Flight 6.296.
Drag Coefficient of the Fuselage and Nacelles 0.01147.
Drag Coefficient of the Wing and Tail Unit 0.00911.

Drag Coefficient of the Airplane:
At the Beginning of Cruising Flight 0.03208.
At Middle of Cruising Flight 0.03064.
Mean Lift Coefficient for the Ceiling Flight 0.45013.

Mean Lift-to-drag Ratio 14.69237.

Landing Lift Coefficient 1.700.

Landing Lift Coefficient (at Stall Speed)2.500
Takeoff Lift Coefficient (at Stall Speed)2.048
Lift-off Lift Coefficient 1.495
Thrust-to-weight Ratio at the Beginning of Cruising Flight 0.615
Start Thrust-to-weight Ratio for Cruising Flight 2.305
Start Thrust-to-weight Ratio for Safe Takeoff 3.142

Design Thrust-to-weight Ratio 3.299

Ratio D r = R cruise / R takeoff 0.734

SPECIFIC FUEL CONSUMPTIONS (in kg/kN * h):
Takeoff 37.5179
Cruising Flight 60.4361
Mean cruising for Given Range 66.0271

FUEL WEIGHT FRACTIONS:

Fuel Reserve 0.04045
Block Fuel 0.28169

WEIGHT FRACTIONS FOR PRINCIPAL ITEMS:

Wing 0.11359
Horizontal Tail 0.00873
Vertical Tail 0.00866
Landing Gear 0.03725
Power Plant 0.09818
Fuselage 0.06829
Equipment and Flight Control 0.12584
Additional Equipment 0.00321
Operational Items 0.01887
Fuel 0.32214
Payload 0.19521

Airplane Takeoff Weight 99035 kg.
Takeoff Thrust Required of the Engine 163.38 kN.
Air Conditioning and Anti-icing Equipment Weight Fraction 0.0217.
Passenger Equipment Weight Fraction
(or Cargo Cabin Equipment)0.0151.
Interior Panels and Thermal/Acoustic Blanketing Weight Fraction 0.0064.
Furnishing Equipment Weight Fraction 0.0130.
Flight Control Weight Fraction 0.0056.
Hydraulic System Weight Fraction 0.0159.
Electrical Equipment Weight Fraction 0.0315.
Radar Weight Fraction 0.0030.
Navigation Equipment Weight Fraction 0.0045.
Radio Communication Equipment Weight Fraction 0.0022.
Instrument Equipment Weight Fraction 0.0052.
Fuel System Weight Fraction 0.0096.

Additional Equipment:
Equipment for Container Loading 0.0000.
No typical Equipment Weight Fraction 0.0032.
(Build-in Test Equipment for Fault Diagnosis,

Additional Equipment of Passenger Cabin)

TAKEOFF DISTANCE PARAMETERS

Airplane Lift-off Speed 300.62 km/h.
Acceleration during Takeoff Run 2.65 m/s*s.
Airplane Takeoff Run Distance 1313 m.
Airborne Takeoff Distance 578 m.
Takeoff Distance 1892 m.

CONTINUED TAKEOFF DISTANCE PARAMETERS

Decision Speed 285.59 km/h.
Mean Acceleration for Continued Takeoff on Wet Runway 0.42 m/s*s.
Takeoff Run Distance for Continued Takeoff on Wet Runway 1975.57 m.
Continued Takeoff Distance 2553.94 m.
Runway Length Required for Rejected Takeoff 2643.97 m.

LANDING DISTANCE PARAMETERS

Airplane Maximum Landing Weight 75059 kg.
Time for Descent from Flight Level till Aerodrome Traffic Circuit Flight 20.4
min.
Descent Distance 49.23 km
Approach Speed 263.93 km/h.
Mean Vertical Speed 2.10 m/s.
Airborne Landing Distance 523 m.
Landing Speed 248.93 km/h.
Landing run distance 785 m.
Landing Distance 1308 m.
Runway Length Required for Regular Aerodrome 2184 m.
Runway Length Required for Alternate Aerodrome 1857 m.

Appendix B

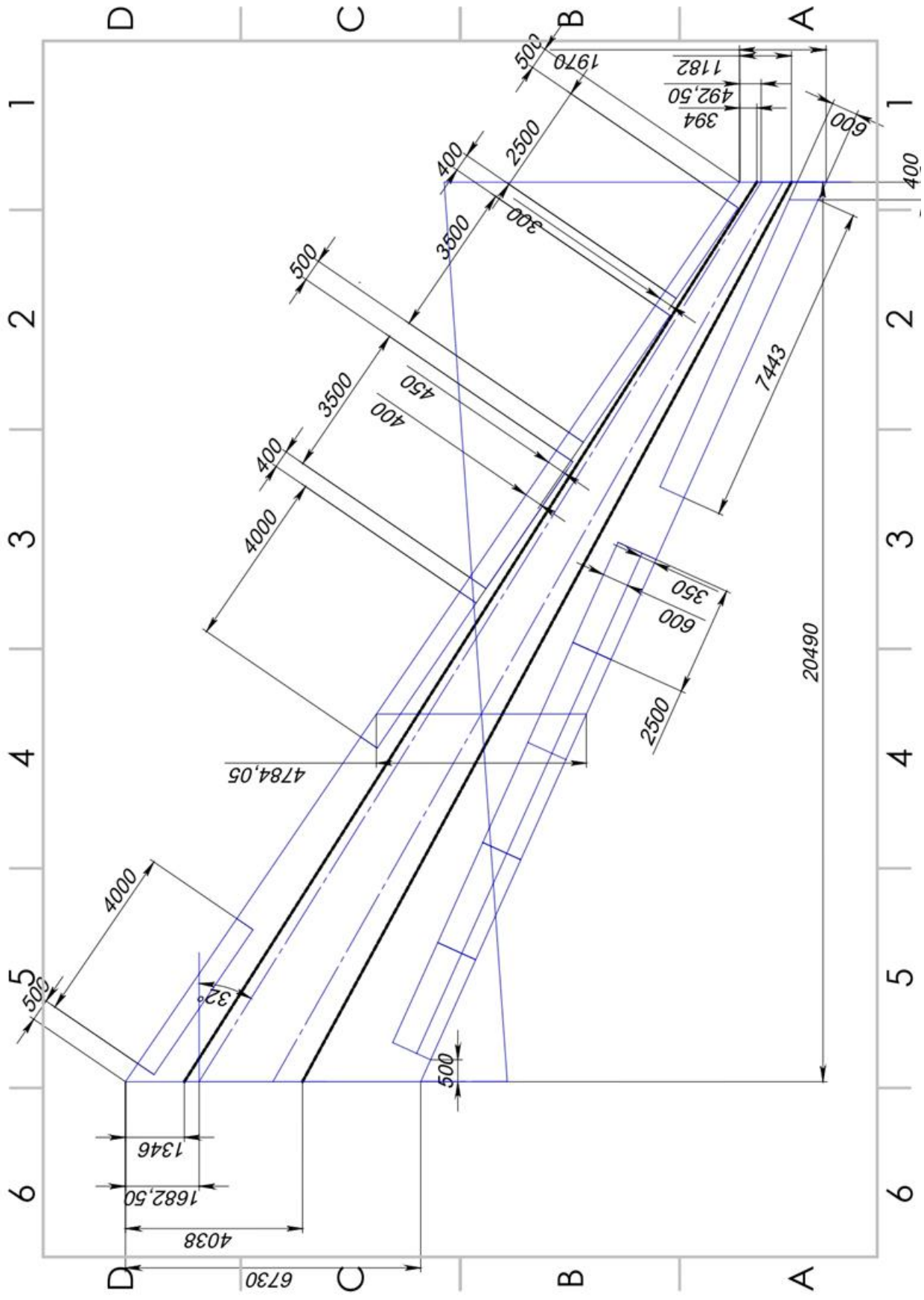
A
B
C
D
1
2
3
4
5
6
500
1970
1182
492,50
394
600
400
2500
400
3500
300
500
7443
3500
450
400
400
4000
350
600
2500
20490
4784,05
4000
500
32°
500
1346
1682,50
4038
6730

Appendix C